





**A TRIBUTE TO EDWARD P. GLENN (1947–2017):
A LEGACY OF SCIENTIFIC ENVIRONMENTAL
ASSESSMENT AND APPLICATIONS IN HYDROLOGICAL
PROCESSES**

Climate sensitivity of water use by riparian woodlands at landscape scales

Marc Mayes¹  | Kelly K. Caylor^{1,2,3} | Michael Bliss Singer^{1,4,5}  |
John C. Stella⁶  | Dar Roberts⁶ | Pamela Nagler⁷ 

¹Earth Research Institute, University of California-Santa Barbara, Santa Barbara, California

²Department of Geography, University of California-Santa Barbara, Santa Barbara, California

³Bren School of Environmental Science and Management, University of California-Santa Barbara, Santa Barbara, California

⁴School of Earth and Environmental Sciences, Cardiff University, Cardiff, UK

⁵Water Research Institute, Cardiff University, Cardiff, UK

⁶Department of Sustainable Resources Management, SUNY College of Environmental Science and Forestry, Syracuse, New York

⁷U.S. Geological Survey, Southwest Biological Science Center, Tucson, Arizona

Correspondence

Marc Mayes, Earth Research Institute, University of California-Santa Barbara, Santa Barbara, CA 93106.

Email: mmayes@ucsb.edu

Funding information

National Science Foundation, Grant/Award Numbers: BCS-1660490, EAR-1700517, EAR-1700555; Strategic Environmental Research and Development Program, Grant/Award Number: RC18-1006

Abstract

Semi-arid riparian woodlands face threats from increasing extractive water demand and climate change in dryland landscapes worldwide. Improved landscape-scale understanding of riparian woodland water use (evapotranspiration, ET) and its sensitivity to climate variables is needed to strategically manage water resources, as well as to create successful ecosystem conservation and restoration plans for potential climate futures. In this work, we assess the spatial and temporal variability of Cottonwood (*Populus fremontii*)-Willow (*Salix gooddingii*) riparian gallery woodland ET and its relationships to vegetation structure and climate variables for 80 km of the San Pedro River corridor in southeastern Arizona, USA, between 2014 and 2019. We use a novel combination of publicly available remote sensing, climate and hydrological datasets: cloud-based Landsat thermal remote sensing data products for ET (Google Earth Engine EEFlux), Landsat multispectral imagery and field data-based calibrations to vegetation structure (leaf-area index, LAI), and open-source climate and hydrological data. We show that at landscape scales, daily ET rates (6–10 mm day⁻¹) and growing season ET totals (400–1,400 mm) matched rates of published field data, and modelled reach-scale average LAI (0.80–1.70) matched lower ranges of published field data. Over 6 years, the spatial variability of total growing season ET (CV = 0.18) exceeded that of temporal variability (CV = 0.10), indicating the importance of reach-scale vegetation and hydrological conditions for controlling ET dynamics. Responses of ET to climate differed between perennial and intermittent-flow stream reaches. At perennial-flow reaches, ET correlated significantly with temperature, whilst at intermittent-flow sites ET correlated significantly with rainfall and stream discharge. Amongst reaches studied in detail, we found positive but differing logarithmic relationships between LAI and ET. By documenting patterns of high spatial variability of ET at basin scales, these results underscore the importance of accurately accounting for differences in woodland vegetation structure and hydrological conditions for assessing water-use requirements. Results also suggest that the climate sensitivity of ET may be used as a remote indicator of subsurface water resources relative to vegetation demand, and an indicator for informing conservation management priorities.

KEYWORDS

climate, conservation, ecosystem management, evapotranspiration, remote sensing, riparian woodlands, San Pedro River, water

1 | INTRODUCTION

In semi-arid landscapes, riparian woodlands are biodiversity hotspots, serving as moisture and thermal refugia for many species, whilst providing important ecosystem services for people, ranging from food and water to cultural value and recreation (Albright et al., 2017; Jones et al., 2010; Seavy et al., 2009; Stella, Rodríguez-González, Dufour, & Bendix, 2013). Most overstory tree species in riparian woodlands are obligate or facultative phreatophytes, meaning they depend on access to soil and shallow groundwater resources near stream channels for survival (Eamus, Zolfaghar, Villalobos-Vega, Cleverly, & Huete, 2015; Grime, 1977; Ohmart, Anderson, & Hunter, 1988; Smith, Devitt, Sala, Cleverly, & Busch, 1998). Globally, riparian woodlands face threats from extractive water-use related to land-use practises (groundwater pumping, stream diversion) and from climate change (Stella & Bendix, 2018). Altered rainfall regimes modify streamflow dynamics, which together affect water table elevations and change seasonal dynamics of soil water availability (Shafroth, Stromberg, & Patten, 2002; Singer et al., 2014; Stromberg, Tluczek, Hazelton, & Ajami, 2010). Increasing air temperatures and lengthening temperature-cued growing seasons result in higher instantaneous and growing season-integrated atmospheric water demand, which can increase plant water demand and water loss via evapotranspiration (ET) (Serrat-Capdevila, Scott, James Shuttleworth, & Valdés, 2011; Zhang et al., 2015).

As riparian ecosystems receive increasing attention as ribbons of biodiversity within arid environments and a conservation priority, it is critical to improve understanding and monitoring of hydrological processes determining riparian zone water balance. These hydrological processes can be categorized by those that affect water supply to the riparian zone, and those that comprise water loss or demand. Supply processes include mountain-front recharge dynamics (Wilson & Guan, 2004) and water retention dynamics of shallow aquifer units and riparian-zone soils shaped by geological and climate variables (Gungle et al., 2019). Water loss or demand processes include vegetation water use (ET), and land-use related water extraction from groundwater pumping or stream diversions. Interactions amongst water supply and demand processes organize natural gradients of water availability along reach and channel sections. These gradients of water availability are reflected in variables such as streamflow permanence (i.e., perennial vs. intermittent flow) and the corridor-scale spatial distribution of vegetation types from xerophytes to large deciduous trees. Generally, overstory riparian woodland species in semi-arid ecosystems are adapted to year-round conditions of high soil moisture and intolerant of dry soil conditions, and as such are concentrated spatially near stream channels or springs where high soil moisture persists; when soil moisture becomes limiting they close stomata and down-regulate water and CO₂ exchange. (i.e., isohydric behaviour) (Hultine et al., 2020; McDowell et al., 2008).

It remains difficult to monitor changes in water availability relative to riparian vegetation demand across riparian corridors at large scales (10s–100s km). Understanding of the spatial and temporal variability of riparian vegetation ET in relation to vegetation structure and the

sensitivity of ET to climate variables across corridors also remains poor (Williams & Scott, 2009). Improved quantification of riparian vegetation ET and its sensitivity to climate variables are vital to ascertain ecosystem responses to potential climate futures involving changing rainfall regimes (Diffenbaugh, Swain, Touma, & Lubchenko, 2015; Polade, Gershunov, Cayan, Dettinger, & Pierce, 2017; Singer & Michaelides, 2017) and increasing aridity (Cayan et al., 2010; Seager et al., 2007). In the future, the spatial distribution of riparian areas with sufficient subsurface water resources to support phreatophytic vegetation communities, for example, may decline across many dry-land regions, making some regions less suitable than others as “refugia” for conservation or restoration (McLaughlin et al., 2017; Stella, Riddle, Piégay, Gagnage, & Trémélo, 2013). Developing spatially explicit understanding of the variability of ET and indicators of water availability in riparian zones could also inform goals and designs of conservation and/or restoration plans to match hydrologic conditions of heterogeneous riparian vegetation communities at reach scales (Perry, Reynolds, Beechie, Collins, & Shafroth, 2015; Ramírez-Hernández, Rodríguez-Burgueño, Zamora-Arroyo, Carreón-Diazconti, & Pérez-González, 2015; Schlatter, Grabau, Shafroth, & Zamora-Arroyo, 2017).

Here, we assess the spatial and temporal variability of semi-arid riparian woodland ET, and its relations to climate variables along a major river corridor in the Southwest USA, using a novel combination of remote sensing data products and hydrological data. Often, large-scale evaluations of vegetation ecological function in ecosystem models— including use and exchange of carbon, nutrient and water resources (e.g., ET), and other biophysical interactions—make two simplifying assumptions. The first is that a given vegetation type at a certain demographic or successional stage responds similarly to climate and disturbance across space (Camporeale, Perucca, Ridolfi, & Gurnell, 2013). The second assumption is that relationships between ecological function and canopy structure—physical attributes of vegetation stands such as leaf area per unit ground area (leaf-area index, LAI)—remain more or less constant (Nagler, Morino, Murray, Osterberg, & Glenn, 2009). We examine these assumptions by studying relationships of riparian vegetation community ET to climate variables (rainfall, temperature), and relationships of vegetation function (ET) to canopy structure (LAI), across a series of stream sites with perennial and intermittent streamflow representing a gradient of water availability. For this study, we focus on ET for overstory, “gallery” riparian woodland vegetation communities dominated by cottonwood (*Populus*) and willow (*Salix*) species within the San Pedro River corridor in southeastern Arizona, USA.

Characterization of ET dynamics for riparian gallery woodlands using field data has been limited in spatial and temporal extent due to logistical challenges the system poses for existing methods, including eddy covariance flux towers and individual tree-based observations (sap flux, leaf porometry). Riparian woodland communities grow in narrow, heterogeneous stands along stream channels that often do not meet spatial requirements for accurate flux tower measurements (Baldocchi et al., 2001). Their tall canopies (>20 m) also require significant infrastructure investment for sensor setup above the canopy.

One of few published flux-tower-derived ET datasets for riparian gallery woodlands, on the Middle Rio Grande River, measured total annual ET over multiple years between 950 and 1,230 mm for mature (25 m tall) cottonwood-dominated stands (Cleverly et al., 2015; Dahm et al., 2002). Flooding regime was noted as important variables affecting stand-level ET dynamics (Cleverly et al., 2015). Another flux-tower based ET study on the Consumes River in California quantified cumulative annual ET of 1,095 mm for riparian cottonwoods and noted sensitivity of CO₂ uptake and ET to groundwater depth (Kochendorfer et al., 2011). Although their location in a more northern, mesic climate zone with a shorter growing season makes growing season ET totals difficult to compare, other studies combining flux-tower and leaf-scale observations of riparian woodland transpiration on the Platte River in Nebraska reported daily ET rates of 0–8 mm day⁻¹ for cottonwood and 0–10 mm day⁻¹ for willow at a single observational site (Irmak et al., 2013; Kabenge & Irmak, 2012). Ultimately flux tower measurements are point-based observations that alone are difficult to scale across lengths of major riparian corridors.

Field studies assessing ET dynamics of sets of individual trees amongst stream sites or channel positions provide some insight into spatial variability of gallery woodland ET, but with limited site replication, and often only 1–2 years of data, they are insufficient to investigate multi-year vegetation structure-ET and climate-ET relationships comprehensively at scales of 10¹–10² km long riparian corridors. Studies using sapflow sensors to quantify mature gallery woodland ET on the San Pedro have documented a range of total growing season ET from 484 mm at an intermittent-streamflow site (Boquillas) to 966 mm at a perennial-streamflow site (Lewis Springs) (Gazal, Scott, Goodrich, & Williams, 2006). In addition significant variability in daily ET rates (3–6 mm day⁻¹) across early and advanced-successional riparian woodland patches has been documented (Schaeffer, Williams, & Goodrich, 2000). One study that capitalized on reservoir maintenance to measure cottonwood and willow physiological responses to reduced subsurface water availability found significant negative responses of sapflow, leaf water potential and tree-ring width to reduced volumetric soil moisture coincident with draining, and rebound of sapflow and leaf-water potential upon soil moisture recovery with reservoir refilling (Hultine, Bush, & Ehleringer, 2010). This work demonstrates that riparian woodland ET can be highly sensitive to interannual changes in water availability with important variations by species.

Remote sensing observations have proved to be key tools for upscaling point-based and field site-level findings on cottonwood-willow gallery woodland ET to landscape-scale understanding and monitoring capability. Two general approaches have been used with satellite and airborne sensors: a correlative approach linking flux tower observations to visible-near infrared (VNIR) imagery, and surface energy-balance approaches using thermal image data. The first develops relationships between flux tower data on vegetation water exchange, and vegetation indices (VIs) derived from MODIS and Landsat VNIR satellite data, to scale point-based flux-tower estimates of vegetation ET to riparian corridor and landscape scales

(Nagler et al., 2005; Nagler et al., 2005; Nagler et al., 2009; Scott et al., 2008). The VIs used in flux tower-VNIR image data correlations, such as Normalized Difference Vegetation Index (NDVI) and Enhanced Vegetation Index (EVI), are widely applicable over long-term Landsat and MODIS image archives, but depend on having flux tower data available for vegetation types of interest for calibration. These methods also assume that ecosystem water-flux dynamics measured at limited locations and time periods are representative of large areas (Glenn, Nagler, & Huete, 2010). Using VIs to model ET in a given landscape also means that the same VNIR imagery cannot be used to independently measure and model vegetation structure, such as biomass or LAI, in order to explore variations in the relationships between vegetation structure and ET across stream reach and landscape positions. Such relationships may identify important differences in vegetation function, such as ET per unit leaf area that may differ amongst stands with consequence for identifying signals of vegetation water-use efficiency or stress at community scales (Hultine et al., 2010; Watson, Vertessy, & Grayson, 1999).

The second remote sensing approach, surface energy-balance modelling, uses thermal infrared (TIR) image data on surface temperatures in combination with local and/or spatially modelled meteorological data to estimate latent heat fluxes (Allen, Tasumi, & Trezza, 2007; Anderson et al., 2011; Bastiaanssen et al., 2005; Senay, 2018; Senay et al., 2013). Over vegetated areas, this latent heat flux is dominated by ET. An advantage of surface energy-balance modelling is that it assumes no fixed relationship between indicators of vegetation structure and ET within or across vegetation types. However, surface energy-balance modelling does require more extensive meteorological data and computational resources to complete and also involves region-specific model tuning in many areas (Senay et al., 2013). Recent advances, such as the development of cloud-computing in platforms like Google Earth Engine, are increasing the accessibility of the ancillary data and computing power needed to estimate ET via surface energy-balance methods across large volumes of satellite imagery. Example products include Landsat-METRIC model (Mapping ET with Internalized Calibration)-based actual ET (ET_a) product calculated with supporting meteorological data in Google Earth Engine (Allen et al., 2015).

We characterized multi-year ET dynamics of riparian gallery woodlands in the San Pedro River (SPR) across 80 km of the riparian corridor, and tested relationships of total growing season ET to seasonal climate variables and vegetation structure (NDVI, LAI) at four sites spanning a gradient in streamflow conditions. We analysed relationships amongst ET and riparian vegetation structure in a novel way by combining independent surface energy-balance derived remote sensing datasets for ET (Google Earth EEFlux) and Landsat VI-derived LAI estimates, using specific relationships developed for cottonwood-willow vegetation types (Nagler, Glenn, Lewis Thompson, & Huete, 2004). Our working hypotheses were the following:

- Gallery woodland ET across the basin correlates positively to shallow subsurface water availability and canopy leaf area (LAI) across stream sites. We used stream discharge and streamflow

permanence status (perennial vs. intermittent flow) as proxy variables for subsurface water availability.

- The sensitivity of gallery woodland ET to seasonal climate variables (temperature, rainfall) differs according to streamflow permanence status. At stream sites with perennial flow, we predicted positive correlations of ET with temperature, where high subsurface water availability relative to vegetation demand would permit increased woodland tree water-use tradeoffs in up-regulation of CO₂ assimilation. Conversely at intermittent-flow sites, we predicted positive ET correlations to rainfall and stream discharge, where lower subsurface water availability relative to vegetation demand would make vegetation ET more sensitive to additional water inputs.

Our assessment addressed the questions of how climate variables by season affect riparian woodland ET dynamics across gradients of stand structure and subsurface water availability. We also discuss the potential of using remote indicators of gallery woodland functional response to climate (*sensu* Hultine et al., 2020) as a clue for

diagnosing subsurface water-resource availability relative to vegetation demand, with potential application for informing riparian corridor conservation and environmental monitoring.

2 | METHODS

2.1 | Study region

The Upper San Pedro River (SPR) watershed in Cochise County, AZ and Sonora, Mexico is one of few free-flowing (undammed) rivers in the southwestern US (Figure 1). The climate is semi-arid with large seasonal and diurnal temperature variability and mean annual rainfall of 300–400 mm yr⁻¹; about 60–70% of rain falls in summer monsoon periods, and the rest in winter and spring frontal storms (Scott et al., 2008). A progressive decline in monsoonal streamflow over a multidecadal period has been observed, but it cannot be attributed to any observed trends in rainfall (Goodrich et al., 2008; Singer &

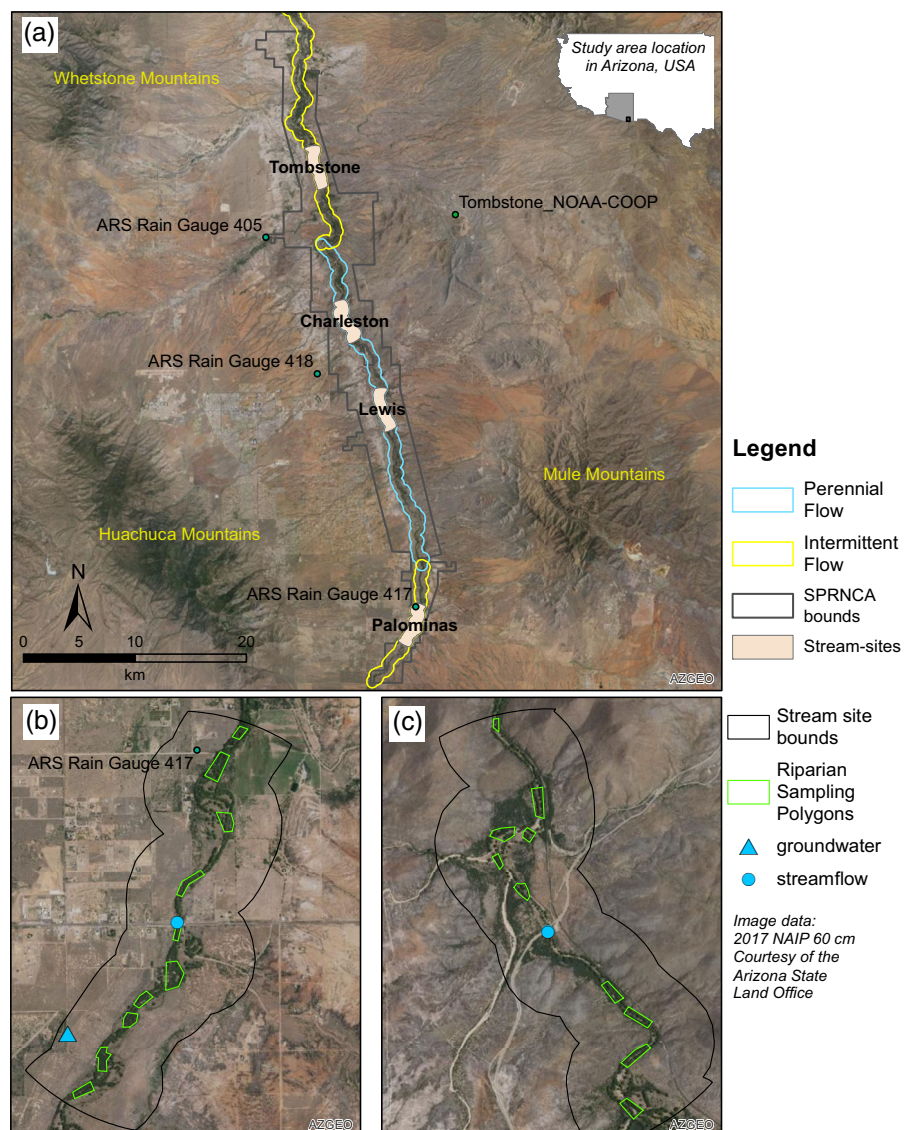


FIGURE 1 San Pedro River study region, southeastern Arizona. An overview map locates overstory riparian woodland sites of focus to this study in pink, perennial and intermittent-flowing stream sections, and sites of NOAA-COOP climate data and local rainfall gauges (USDA Agricultural Research Service (ARS)) (Panel A). The river flow direction is south to north. Panels B and C show close-up views of 4 km stream-sites with intermittent flow (Palominas, B) and perennial flow (Charleston, C)

Michaelides, 2017; Thomas & Pool, 2006). Differences in upslope geologic structure, floodplain aquifer composition and thickness drive variations in shallow subsurface water availability to ecosystems along the riparian corridor (MacNish, Baird, & Maddock III, 2009). Riparian vegetation communities along the upper SPR include gallery overstory woodlands dominated by Fremont Cottonwood (*Populus fremontii*) and Gooddings Willow (*Salix gooddingii*), mesquite woodland (*Prosopis velutina*), sacaton grassland (*Sporobolus airoides*, *Sporobolus wrightii*), Cienega wetlands and riverine marshlands and xeroriparian shrublands (Makings, 2005). Significant changes have occurred in vegetation distribution in the last 150 years due to stream entrenchment, driven by climate variability and land-use activities (Stromberg et al., 2010). Population and development are expanding in nearby towns of Sierra Vista and Benson, associated with activity at the Fort Huachuca United States Army base and establishment of bedroom and retirement residential communities. Agriculture and ranching are also longstanding land-use activities. Historical and current groundwater demand, combined with potential for housing development in the future, have been of concern for maintaining river baseflow and subsurface water resources since the 1980s. The San Pedro Riparian National Conservation Area (SPRNCA), extending roughly 50 km from the US-Mexico border to the town of St. David, was established by Congress in 1988 to conserve, protect and enhance the riparian area.

This study focuses on cottonwood-willow dominated riparian gallery woodlands. Gallery woodlands are located along active and secondary channels of the river in communities in stands from 1–10 ha 10^0 – 10^1 ha in area (Nguyen, Glenn, Nagler, & Scott, 2015; Stromberg et al., 2006). The specific study reach has perennial flow for most of its central length, with intermittent/seasonal flow at the north and south ends (Leenhouts, 2006; MacNish et al., 2009) (Figure 1). Over the last century there have been complex changes in gallery woodland stand extent and locations in the upper SPR related to interactions of early-20th century flooding, feedbacks of grazing and other land-uses on erosion and vegetation disturbances, entrenchment and groundwater extraction (Stromberg et al., 2010). Increases in SPR gallery woodland area upstream have been shown to directly and positively correlate with migratory bird populations (Krueper, Bart, & Rich, 2003) and likely with various reptiles and amphibians. Since the

1980s, concerns have mounted for gallery woodland health as a result of the impact of continued groundwater extraction alongside increasing air temperatures and changing rainfall distributions (Seager et al., 2007; Singer & Michaelides, 2017).

2.2 | Gallery woodland vegetation community sampling

Data on riparian woodland stand structure and ET were extracted from satellite image data and derived products based on site visits in 2019 and sites of prior research with supporting field data on the San Pedro (Leenhouts, Stromberg, & Scott, 2006). We focused our analysis on four subreaches (stream sites) with available data on streamflow and groundwater distributed across the SPRNCA: Palominas, Lewis Springs, Charleston and Tombstone (Figure 1). For generalization, we classify and refer to these sites by relative position along the stream-channel and streamflow permanence status (Table 1). Lewis Springs and Charleston had perennial streamflow whilst Palominas and Tombstone had intermittent streamflow; riparian overstory woodlands at all stream sites consisted predominantly of cottonwood and willow trees (Table 1). To control for the geographic extent of vegetation community sampling relative to discharge data, stream-site boundaries were generated by centering a 4 km² polygon on stream gauges that were 4 km in length with a 0.5 km buffer on either side of the stream channel (Figure 1). Within each of the stream sites, we created 10 sampling polygons over gallery woodland stands for subsequent remote sensing analyses of ET, LAI and their relationships with hydrological and climate data (Figure 1 panels B and C). These sampling polygons were chosen based on site visits, GPS points taken in March 2019, and inspection of high-resolution NAIP (National Agricultural Imagery Program, USDA-FSA Aerial Photography Office) aerial imagery from 2017 with 60 cm pixel resolution, imported as basemap in ArcGIS 10.5.1 courtesy of the Arizona State Land Office. Using the high-resolution NAIP imagery overstory cottonwood-willow stands were readily identifiable against potential confounding vegetation types, such as dense mesquite stands, based on crown shapes, sizes and shadowing. Finally sampling polygons were checked against time

TABLE 1 Stream-sites of primary focus along the San Pedro River presented in upstream-to-downstream order

Site name	Categorization for this study <i>Abbreviation in italics</i>	Streamflow permanence ^a	Cottonwood/willow importance value (%) amongst woodland trees ^b
Palominas	Intermittent flow—upstream <i>I-U</i>	Intermittent-wet	65
Lewis Springs	Perennial flow—upstream <i>P-U</i>	Perennial flow	100
Charleston	Perennial flow—Downstream <i>P-D</i>	Perennial flow	88
Tombstone	Intermittent flow—downstream <i>I-D</i>	Intermittent-wet	91

^aAs categorized from data in Leenhouts, 2006, Chapter B p. 40–43, in USGS Scientific Investigations Report 2005–5,163.

^bImportance value for all age classes of cottonwood and willow trees calculated based on relative abundance, in terms of stem density and basal area, as indicated by Stromberg, Lite, Dixon, Rychener, and Makings (2006), Chapter C p. 88, Table 29, in USGS Scientific Investigations Report 2005–5,163.

series imagery in Google Earth Pro to verify the stability of vegetation cover for purposes of these analyses.

2.3 | Local climate and hydrological datasets

Climate data including air temperature and rainfall were obtained from the Tombstone NOAA-COOP station (GHCND:USC00028619) via the National Climatic Data Center (renamed National Centers for Environmental Information) web site and analysed for the period 1960-present, encompassing two 30-year periods. Additional rainfall data, closer to studied stream-sites, were obtained from USDA-Agricultural Research Service (ARS) stream gauges 405, 417 and 418 (<https://www.tucson.ars.ag.gov/dap/digital/aggregate.asp>). Rainfall data were summed and analysed monthly and seasonally (Winter = Nov–Feb; Pre-Monsoon = March–June; Monsoon = July–October) according to the local hydrologic year from Nov 1–Oct 31 (Scott et al., 2008). Temperature data were analysed for trends in daily maximum and minimum temperatures to study relationships between climate extremes and gallery woodland ET dynamics. Hydrologic data were obtained from the USGS-National Water Information Service via the dataRetriever package in R developed by the USGS (De Cicco, Hirsch, Lorenz, & Watkins, 2018). These included streamflow data for three of the stream sites and groundwater levels for the closest wells to stream gauges (within 500 m of the stream channel) with data covering the period 2000-present (Table S1).

2.4 | Remote sensing datasets: ET and vegetation structure (NDVI, LAI)

2.4.1 | Total annual ET: EEFlux

Actual Evapotranspiration raster data (ET_a) were downloaded from the EEFlux platform on Google Earth Engine, which uses a version of the METRIC (Mapping ET with Internalized Calibration) model to calculate daily ET rates using Landsat thermal image data and supporting meteorological data (Allen et al., 2007; Allen et al., 2015). We focused on hydrologic years with complete Landsat 8 records—2014 to 2019—and obtained 10–17 ET rasters per year (Table S2). Between 9 and 13 rasters spanning the extent of the growing season of cottonwood-willow overstory vegetation were subset from annual records. Total growing season ET was calculated for each year using a spline-integration method (area-under-curve function in the MESS package for R [Ekstrom, 2019]) at pixel level (30 m) between days-of-year (DOY) corresponding with March 1 and October 31. We plotted rasters for total growing season ET (mm) and mean 6-year total growing season ET for the San Pedro riparian corridor, and visualized patterns of 6-year mean total annual ET against stream profile elevation data extracted from the ASTER digital elevation model (ASTER-GDEM Version 3, NASA/METI 2019) with 30 m pixel resolution. Finally, we extracted median ET for sampling polygons across stream sites for further analysis.

2.4.2 | Vegetation structure

Vegetation structure (LAI) was assessed using NDVI calculated from Landsat 8 satellite data, and field data-based calibrations of NDVI to cottonwood/willow LAI from remote sensing studies on the lower Colorado river (Nagler et al., 2004). These NDVI-LAI calibrations from the early 2000s were developed with Landsat 7 NDVI; therefore, it was necessary to back-scale Landsat 8 reflectance values to Landsat 7 equivalent NDVI values (see Appendix S1 for details; Figure S1 for Landsat 7-Landsat 8 NDVI relationships). Six Landsat 8 OLI images (WRS path 035/row 038) were acquired for years 2014–2019 corresponding with years for which EEflux ET data were obtained (Table S3). These Landsat 8 images were acquired during the late pre-monsoon period (May–June) in order to quantify gallery woodland overstory vegetation structure after leaf-out, but before additional greening of understory grasses and shrubs during the monsoon rains that can complicate interpretation of overstory versus understory contributions to pixel reflectance. Four Landsat 7 images were acquired with similar seasonal timing for years 2014–2018 (Table S3) to develop scaling relationships between the sensors (see Appendix S1 and Table S4). All images were located and downloaded using GLOVIS, ESPA and Python bulk-download utilities developed and supported by USGS. NDVI was calculated using the standard formula as the normalized difference between near-infrared reflectance (P_{nir}) and red reflectance (P_{red}) (Equation (1)):

$$NDVI = \frac{P_{nir} - P_{red}}{P_{nir} + P_{red}} \quad (1)$$

We estimated LAI of gallery woodland stands by using relationships between NDVI, the fraction of canopy intercepted radiation (fIRs), and light-extinction coefficients (k) derived from field measurements and aerial multispectral imagery over riparian woodlands and restoration plots in the lower Colorado River basin (Nagler et al., 2004). Median NDVI values were extracted for riparian gallery woodland stand-polygons, and we calculated fIR based on Equation (2) and LAI from rearranging an equation derived for k based on fIRs and LAI (Equation (3)):

$$fIRs = 1.61 * NDVI + 0.12 \quad (2)$$

$$LAI = -\frac{\ln(1 - fIRs)}{k} \quad (3)$$

We modelled stand-level k as in Equation (4), computed as a weighted mean of k -values reflecting mixtures of cottonwood-like ($k = 1.25$) and willow-like (0.60) canopy architecture as characterized on the lower Colorado. k -Values were calculated for ranges of cottonwood and willow qualitatively bracketed by ranges of importance values documented in field surveys (Stromberg, Lite, Dixon, et al., 2006):

$$k_{\text{canopy}} = f_{\text{cottonwood}} * k_{\text{cottonwood}} + f_{\text{willow}} * k_{\text{willow}} \quad (4)$$

From these models (see Appendix S1 and Table S5), a k_{canopy} value of 0.99 was chosen for modelling canopy LAI for all stream sites. This determination was made based via comparisons of calculated stream site average LAI estimates to field-reported LAI values of 1.5–3 for mature riparian woodland stands on the San Pedro (Gazal et al., 2006; Schaeffer et al., 2000). Finally, we extracted median NDVI and LAI for sampling polygons across stream sites for further analysis.

2.5 | Analysis

The main objectives of our analyses were to quantify the spatial and temporal variability of (1) gallery riparian woodland ET; (2) vegetation structure (LAI); (3) relationships between riparian woodland ET and hydro-climate variables and (4) variability in riparian woodland structure (LAI)–function (ET) relationships across stream sites with differing subsurface water availability as characterized by streamflow permanence status. Prior to the main analyses, we quantified differences in streamflow and streamflow-to-groundwater table elevation relationships amongst sites. For stream sites with available data, we assessed effects of site and hydrologic season on discharge via analysis of variance (ANOVA). Discharge data were natural log-transformed to meet assumptions of normality. Post hoc means comparisons were completed using Tukey's Honest Significant Difference at the 95% confidence level ($\alpha = .05$). Then we conducted regression analyses on discharge and groundwater table elevations by season for the overlapping durations of their data records dating back to 1990. Discharge and groundwater table elevation data were natural log-transformed meet assumptions of normality prior to analyses.

For the first part of our main analysis, we analysed the spatial and temporal variability of riparian woodland ET, NDVI and LAI and quantified their differences by stream site and year. Grouping median values of ET, NDVI and LAI extracted for sampling polygons by stream site ($N = 10$ per stream site), we quantified effects of stream site and year on NDVI, LAI and ET using three ANOVA model structures. These included one and two-factor ANOVA models (site and year individually, year + site) and mixed-effect models with sampling polygon as a random variable. ET, NDVI and LAI data were transformed to meet assumptions of normality prior to analyses using Tukey power-ladder transformations with functions in the R package *rcompanion* (Mangiafico, 2020). Fixed-effect models were compared using r^2 and p values and random effect models using Akaike's Information Criteria (AIC), and post hoc means comparisons were completed using Tukey's Honest Significant Difference at the 95% confidence level ($\alpha = .05$). We quantified and compared the spatial and temporal variability of NDVI, LAI and ET across sites by computing coefficients of variation (CV). We defined spatial CV as the coefficient of variation in metrics (ET, NDVI and LAI) across 10 sampling polygons per site for a given year. We calculated spatial CV by dividing the standard deviation of 10 sampling polygon values per site in a given year by their means,

and taking the average over six hydrologic years (2014–2019). We defined temporal CV as the multi-temporal coefficient of variation of metrics for sampling polygons over 6 years. Multi-temporal CVs were computed by taking the SD of metrics through time for *each* sampling polygon over 6 years, and dividing by that polygon's 6-year mean. Stream site averages of temporal CVs were calculated as the average of all sampling polygon multi-temporal CVs.

For the second part of our main analysis we quantified correlations of total growing season ET and LAI to hydro-climate variables, and relationships of ET to LAI across stream sites. For each stream site, we averaged sampling polygon-level ET and LAI data by year ($N = 10$ sampling polygon values per stream site), and computed Pearson's correlation coefficients of ET and LAI to four hydro-climate variables averaged by season for local hydrologic years 2014–2019, beginning in Nov 2013 and ending in October 2019: total precipitation, daily maximum temperature, daily minimum temperature and stream discharge. Finally, we quantified and compared linear and logarithmic relationships of ET to LAI at the level of sampling polygons across sites to explore the variability of hydrologic function (ET) with respect to stand-level vegetation structure (LAI). Performance across models was compared via Akaike's Information Criteria (AIC).

3 | RESULTS

3.1 | Characterization of hydrological conditions amongst stream sites

Amongst stream sites with perennial and intermittent streamflow, discharge varied markedly by site and season. There were significant effects of site ($F [2,231] = 27.5, p < .001$) and season ($F [2,231] = 81.6, p < .001$) on discharge (overall ANOVA $F [4,231] = 54.7, r^2 = .477, p < .001$). At the downstream-perennial flow site Charleston (D-P), winter and pre-monsoon discharge rates were about double those of intermittent-flow sites (Table 2); means of winter and pre-monsoon discharge rates differed significantly between D-P and the upstream-intermittent flow site Palominas (U-I) but not the downstream-intermittent flow site Tombstone (D-I). Average monsoon discharge rates were significantly higher at the D-I site than both the upstream-perennial flow site Lewis Springs (U-P) and Palominas (U-I) stream sites, whose monsoon discharge rates were similar (Table 2).

During winter and pre-monsoon seasons, stream discharge and groundwater levels correlated significantly for all stream sites. (Figure S2). In the winter season, discharge and groundwater were significantly correlated at all sites with r^2 values between .536–.656. In the pre-monsoon months, Charleston (D-P) had the strongest relationship between discharge and groundwater for any time period or site ($r^2 = .731, p < .01$); at Tombstone (D-I) site the pre-monsoon discharge-groundwater correlation was moderately strong ($r^2 = .571, p < .01$); at Palominas (U-I) the pre-monsoon discharge-groundwater relationship was the weakest amongst stream sites ($r^2 = .301, p < .01$). During monsoon months, correlations of stream discharge to

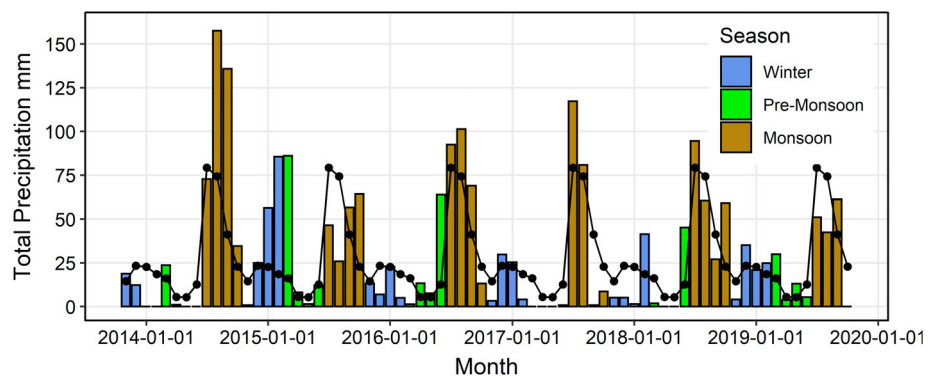
TABLE 2 Mean discharge by season across stream-sites on the San Pedro River, Arizona, 1990–2019 (SD)

Season	Site name (categorization)	Streamflow permanence	N observations	Discharge (SD) ($\text{m}^3 \text{s}^{-1}$)
Winter	Charleston (P-D)	Perennial	137	0.78 (0.165) ^{bd}
	Palominas (I-U)	Intermittent	114	0.26 (0.112) ^e
	Tombstone (I-D)	Intermittent	106	0.36 (0.078) ^{bd}
Pre-monsoon	Charleston (P-D)	Perennial	144	0.24 (0.022) ^{de}
	Palominas (I-U)	Intermittent	111	0.04 (0.018) ^f
	Tombstone (I-D)	Intermittent	102	0.14 (0.018) ^{ce}
Monsoon	Charleston (P-D)	Perennial	147	1.59 (0.242) ^b
	Palominas (I-U)	Intermittent	127	1.87 (0.271) ^b
	Tombstone (I-D)	Intermittent	129	2.57 (0.508) ^a

Note: Categorization codes for sites listed in Table 1.

Note: Discharge values not sharing letters differed significantly in Tukey HSD post hoc means comparisons ($p < .05$).

FIGURE 2 Monthly total rainfall for the San Pedro River region from the Tombstone-NOAA COOP climate station, 2014–2019. Black dots and line over bars indicate 60-yr (1960–2020) monthly averages for reference. Data are organized by hydrologic year corresponding to the preceding annum (e.g., 2014 = Nov. 2013–Oct 2014)



groundwater levels were weakest amongst seasons; Charleston (D-P) and Tombstone (D-I) still had significant discharge-groundwater level correlations but Palominas (U-I) site did not.

3.2 | Climate variability during the study timeframe

During the 6-year study period (2014–2019), total annual and seasonal rainfall varied widely around the 60-year average (1960–2019) at the NOAA-COOP climate station (Figure 2, Table S6). Average total annual rainfall 2014–2019 was 373 (± 49 SD) mm with a coefficient of variation (CV) of 0.22, which was higher than the 60-year average total annual rainfall of 330 (± 87 SD) mm, but with a similar CV (0.26). The pre-monsoon months had the lowest average total rainfall by season, (53 [± 39 SD] mm, CV = 0.74), followed in increasing order by winter months (75 [± 49 SD] mm, CV = 0.66) and monsoon months (246 [± 87] mm, CV = 0.35). The contribution of seasonal rainfall variability to annual totals varied widely by year (Figure 3). The pre-monsoon period had the highest inter-annual variability as shown by CV– in 2017 almost no rain fell during this period, but >100 mm fell in 2014 (Table S6). Compared to the NOAA-COOP climate station, local USDA-ARS rainfall gauges showed similar inter-annual and seasonal patterns of variability (Figure S3).

Daily average maximum and minimum temperatures by month and season during 2014–2019 were 2–4°C higher than 60-year averages and are part of increasing trends in temperatures since 1960 (Figure S4). For 2014–2019, average minimum-maximum daily temperatures were for the winter season 4.99 (± 1.23 SD)°C–18.9 (± 1.30 SD)°C, for the pre-monsoon season 12.9 (± 0.93 SD)°C–29.4 (± 1.36 SD)°C, and for the monsoon season 17.7 (± 0.28 SD)°C–32.0 (± 0.60 SD)°C. Years 2016 and 2017 had multiple winter and pre-monsoon months with average daily maximum temperatures >4°C above 60-year averages, and November 2017 was nearly 6°C above the 60-year monthly average. The year 2019 was relatively cooler than the other years.

3.3 | Spatial and temporal variability of riparian gallery woodland ET and canopy structure

3.3.1 | Patterns in seasonal daily ET rates and total growing season ET at stream sites and at riparian corridor scales

Time series of daily ET rates from 2014 to 2019 across sites, extracted from available Landsat 8-METRIC model ET_a images, captured seasonal patterns of low ET rates (<2 mm day⁻¹) through the

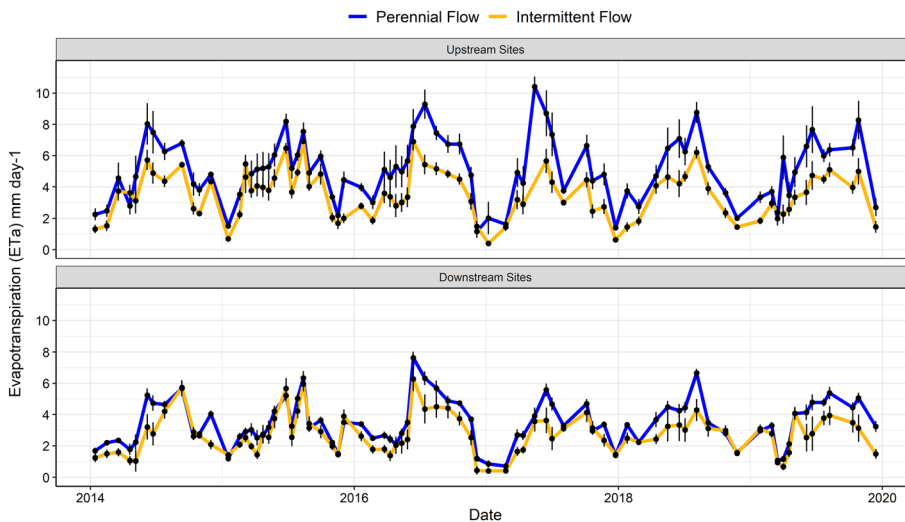


FIGURE 3 Monthly-scale time series of Landsat-8 METRIC model (EEFlux-Google Earth Engine) daily ET compared for perennial and intermittent-flow sites, 2014–2019. Upstream sites are Lewis Springs (perennial flow) and Palominas (intermittent flow). Downstream sites are Charleston (perennial flow) and Tombstone (intermittent flow). Error bars indicate ± 1 SE across 10 sampling polygons per date

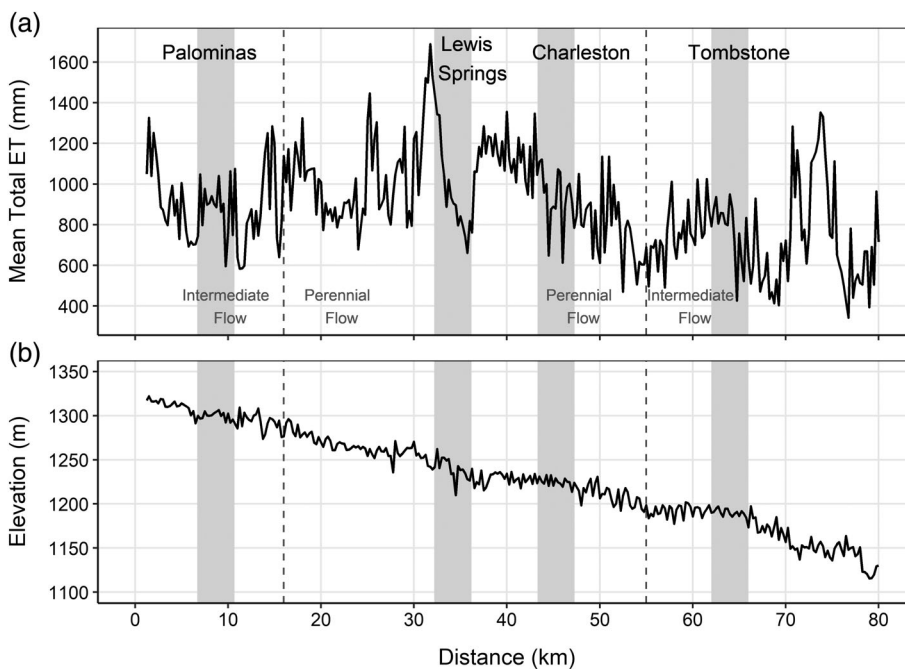


FIGURE 4 Longitudinal profiles of mean 6-year (2014–2019) total growing season ET (a) and elevation (b) along the studied section of the San Pedro River. Stream-sites of 4 km length are indicated by vertical grey bars. Boundaries of perennial and intermittent-flow stream sections in 2018 are indicated by dashed vertical lines and derive from The Nature Conservancy's wet-dry map (see Methods)

winter months, increasing ET rates through the pre-monsoon season, and generally highest daily ET rates in late pre-monsoon or early monsoon periods mid-year (Figure 3). Maximum average daily ET values by year vary from $>10 \text{ mm day}^{-1}$ for the upstream-perennial flow site (U-P, Lewis Springs) in May 2017 to about 6 mm day^{-1} for the downstream-intermittent flow site (D-I, Tombstone) in June 2016. Major temporal patterns in daily ET rates within and amongst years were similar amongst stream sites, as were the inter-annual minima in winter seasons ($0.5\text{--}1.5 \text{ mm day}^{-1}$). Grouped by upstream and downstream positions, the perennial-flow stream sites had higher amplitudes of seasonal variability in ET, with larger increases in ET rates during the pre-monsoon season and maintenance of higher daily ET rates through the monsoon rains, in comparison to the intermittent-flow sites.

Longitudinally along the stream profile from the US-Mexico border (0 km) through the SPRNCA ($\sim 80 \text{ km}$), there was a fourfold range in mean total growing season ET for 2014–2019 ($400 \text{ mm--}1,600 \text{ mm}$) for all vegetation within 60 m of the stream channel centre (thalweg) (Figure 4). Amongst the stream sites, Lewis Springs (U-P) included a region of maximum mean total ET for the whole stream corridor ($\sim 1,600 \text{ mm}$) but with a large decrease in total ET downstream through the stream site. The range of total ET values was similar ($\sim 600\text{--}1,100 \text{ mm}$) longitudinally for the 4 km stream site lengths at Palominas (U-I) and Charleston (D-P) despite their differing flow permanence status. Tombstone (D-I) had the lowest mean total ET amongst the stream sites and was located just upstream of an increase in slope at $\sim 65 \text{ km}$ along the stream profile. Along the section of the SPR corridor studied herein, the perennial-flow

section of the stream, and local ET maxima in perennial and intermittent-flow sections corresponded generally with landscape geological structure known to affect base flow (Gungle et al., 2019) (Figure 1).

3.3.2 | Effects of stream site and year on riparian woodland ET and vegetation structure (LAI, NDVI)

As dependent variables, ET, LAI and NDVI varied significantly by site and year in ANOVA model results. For all dependent variables, stream site accounted for higher proportions of variance than year in one- and two-factor ANOVA models (Table 3). Year alone in one-factor ANOVA did not explain significant variance in ET (Table 3). Mixed-effect ANOVA models indicated significant effects of stream site and year on ET, LAI and NDVI, but also significant random effects of sampling polygons for all variables (see Appendix S2).

Post hoc comparisons of mean ET, LAI and NDVI averaged by stream site for all study years, along with their spatial and temporal coefficients of variability (CV), are reported in Table 4. Spatial variability exceeded interannual variability for ET, LAI and NDVI across sites. Mean total ET for riparian woodlands at Lewis Springs (U-P), 1,414 (± 271 SE) mm, was significantly higher than all other sites ($p < .05$). Mean total ET was similar at Palominas (U-I) (970 [± 187 SE] mm) and Charleston (D-P) (960 [± 120 SE] mm). Mean total ET was significantly lower than all other sites at Tombstone (D-I) (761 [± 184 SE] mm) ($p < .05$). NDVI and LAI trends were similar across sites. Site-level differences were driven by Tombstone (D-I), which had significantly lower NDVI (0.392 [± 0.103 SE]) and LAI (0.80 [± 0.42 SE] $m^2 m^{-2}$) than Palominas (U-I) (NDVI = 0.531 (± 0.072 SE), LAI = 1.46 (± 0.51

SE) $m^2 m^{-2}$) and Lewis Springs (U-P) (NDVI = 0.545 (± 0.105 SE), LAI = 1.67 (± 0.73 SE) $m^2 m^{-2}$). Within all stream sites, the spatial variability (spatial CV) of ET, LAI and NDVI exceeded temporal variability except for ET at Charleston (D-P).

Interannual ET trends differed by site streamflow permanence status, whereas interannual LAI trends differed more strongly by stream site longitudinal position (upstream vs. downstream site location) (Figure 5). For example, regarding ET trends, Lewis Springs (U-P) maintained significantly higher total ET over the study timeframe than Palominas (U-I) despite the sites having similar LAI. For LAI trends, upstream sites Lewis Springs and Palominas had elevated mean LAI in 2015–16 relative to other years, which the downstream sites both lacked. Overall, LAI showed larger temporal variations (temporal CV) than ET. NDVI showed similar interannual trends to LAI (Figure S5).

3.4 | Correlations of ET and LAI to climate variables and discharge across stream sites

There were contrasting trends in relationships of ET to climate and hydrological variables between perennial- and intermittent-flow stream sites (Table 5). At perennial-flow sites, mean total ET correlated to temperature variables. At Lewis Springs (U-P), mean total ET had significant positive correlation with monsoon-season daily maximum temperature ($r = .914$, $p = .011$). At Charleston (D-P), mean total ET showed inverse correlation to monsoon daily minimum temperatures at the 90% confidence level ($\alpha = .10$) ($r = .059$, $p = .059$). In contrast, at intermittent-flow sites, mean total ET correlated to rainfall and stream discharge. Mean total growing season ET at Palominas (U-I) correlated positively with pre-monsoon rainfall as measured by

TABLE 3 Results from fixed-effect analysis of variance models quantifying effects of stream-site (site) and year on evapotranspiration (ET), leaf-area index (LAI) and NDVI for cottonwood and willow-dominated riparian woodlands in the SPRNCA along the upper San Pedro River, Arizona

Dependent variable	Independent variable(s)	F-value (degrees of freedom)	r^2	p
ET	Site	98.6 (3,236)	.551	<.001
	Year	1.99 (5, 234)	.020	.081
	Site + year	Model: 42.8 (8, 231) Site: 106.2 (3) Year: 4.67 (5)	.583	<.001
LAI	Site	39.2 (3, 236)	.324	<.001
	Year	4.7 (5,234)	.072	<.001
	Site + year	Model: 21.3 (8,231) Site: 106 (3) Year: 4.67 (5)	.404	<.001
NDVI	Site	40.5 (3,236)	.332	<.001
	Year	4.5 (5, 234)	.068	<.001
	Site + year	Model: 21.6 (8,231) Site: 45.8 (3) Year: 7.10 (5)	.408	<.001
ET/LAI	Site	26.2 (3, 230)	.245	<.001
	Year	11.0 (5,228)	.177	<.001
	Site + year	Model: 23.0 (8,225)Site: 34.7 (3) Year: 15.9 (5)	.430	<.001

Note: Analyses include data spanning hydrologic years 2014–2019.

Stream-site (<i>categorization</i>)	Mean ET mm	Spatial CV	Temporal CV
Palominas (I-U)	970 ± 187 ^b	0.166	0.083
Lewis Springs (P-U)	1,414 ± 271 ^c	0.187	0.082
Charleston (P-D)	960 ± 120 ^b	0.110	0.129
Tombstone (I-D)	761 ± 184 ^a	0.240	0.093
	Mean LAI (m ² m ⁻²)	Spatial CV	Temporal CV
Palominas (I-U)	1.46 ± 0.51 ^b	0.293	0.149
Lewis Springs (P-U)	1.67 ± 0.73 ^b	0.400	0.210
Charleston (P-D)	1.02 ± 0.28 ^{ab}	0.239	0.201
Tombstone (I-D)	0.80 ± 0.42 ^a	0.502	0.246
	Mean NDVI	Spatial CV	Temporal CV
Palominas (I-U)	0.531 ± 0.072 ^b	0.118	0.085
Lewis Springs (P-U)	0.545 ± 0.105 ^b	0.192	0.075
Charleston (P-D)	0.462 ± 0.053 ^{ab}	0.104	0.074
Tombstone (I-D)	0.392 ± 0.103 ^a	0.254	0.130

Note: Values not sharing letters differed significantly at the 95% confidence level ($p < .05$) in Tukey's Honest Significant Difference post hoc tests.

Note: Categorization of sites by streamflow permanence and relative longitudinal stream position as in Table 1.

the NOAA-COOP climate station ($r = .918$, $p = .010$) and a local ARS rainfall gauge ($r = .950$, $p = .004$). At Tombstone (D-I), total ET correlated positively with rainfall measured at the NOAA-COOP climate station at the 90% confidence level ($\alpha = .10$) ($r = .793$, $p = .060$), and showed an even stronger positive relationship to rainfall measured by the local ARS gauge ($r = .880$, $p = .021$). Tombstone total growing season ET also correlated positively to winter season discharge at the 90% confidence level $\alpha = .10$, $p = .098$.

LAI correlations to hydroclimate variables differed from ET-hydroclimate correlations across sites (Table 6). Instead of contrasts by flow permanence, trends differed between the two upstream sites with higher LAI (Palominas, Lewis Springs) and the two downstream sites with lower LAI (Charleston, Tombstone). At upstream sites LAI correlated positively with pre-monsoon rainfall (Palominas, $r = .859$, $p = .028$; Lewis Springs, $r = .919$, $p = .010$) and inversely with pre-monsoon minimum daily temperatures (Palominas, $r = -.765$, $p = .076$; Lewis Springs, $r = -.910$, $p = .012$). At downstream sites, LAI correlated inversely with pre-monsoon maximum daily temperatures at the 90% confidence level ($\alpha = .10$) (Charleston, $r = -.797$, $p = .058$; Tombstone, $r = -.739$, $p = .093$).

3.5 | Relationships of ET to LAI across stream sites

ET and LAI correlated positively across sampling polygons and stream sites (Figure 6). Pooled across all sites, linear and natural-logarithm models performed similarly for predicting ET from LAI (linear model, $ET = 548.9 + 386.2 \cdot LAI$, $F(1,238) = 337.4$, $r^2 = .585$, $p < .001$; logarithmic model $ET = 985.4 + 463.1 \cdot \ln(LAI)$, $F(1,238) = 336.5$, $r^2 = .584$, $p < .001$). At individual stream sites, however, logarithmic models outperformed linear models for predicting ET as a function of LAI

TABLE 4 Comparisons of mean evapotranspiration (ET), leaf-area index (LAI) and Normalized Difference Vegetation Index (NDVI) at stream-sites along the San Pedro River, Arizona, for the 2014–2019 hydrologic years

(Table S7). Grouped by flow status, slope coefficients were higher for upstream sites than downstream sites. Amongst the perennial-flow stream sites the ET-LAI relationship was stronger for the upstream site (Lewis Springs) with a LAI range of 3.5 m² m⁻² compared to the downstream site with an LAI range of 1.75 m² m⁻². (Figure 6a vs. 6c). ET-LAI logarithmic relationships were similar for intermittent flow sites at upstream and downstream sites (Figure 6b vs. 6d). NDVI relationships to ET were similar to ET-LAI relationships (Figure S6).

Ratios of ET to LAI differed significantly across sites and years (Figure 7). Patterns in interannual variability differed by site flow status. For perennial-flow sites, ET/LAI at both Lewis Springs (U-P) and Charleston (D-P) increased in 2017–2018, years with lower pre-monsoon rainfall compared to study period means. ET/LAI at intermittent-flow sites had little interannual variability at Palominas (U-I), but high interannual variability and intra-site variability at Tombstone (D-I). Averaged by site for all years, mean ET/LAI ratios of upstream sites Palominas (U-I) (693, 95% CI 642–747) and Lewis Springs (U-P) (857, 95% CI 791–927) differed significantly from each other ($p < .05$, Tukey HSD tests). The mean ET/LAI ratios of the downstream sites Charleston (D-P) (961, 95% CI 891–1,036) and Tombstone (D-I) (1,051, 95% CI 975–1,133) were not significantly different from each other.

4 | DISCUSSION

The results of this study counter two common assumptions made about ecological functioning of a given (single) vegetation type at landscape scales. Representations of plants in hydrological and land surface models often assume that: (1) ecological function of a given vegetation type, such as ET, responds similarly to external forcing like

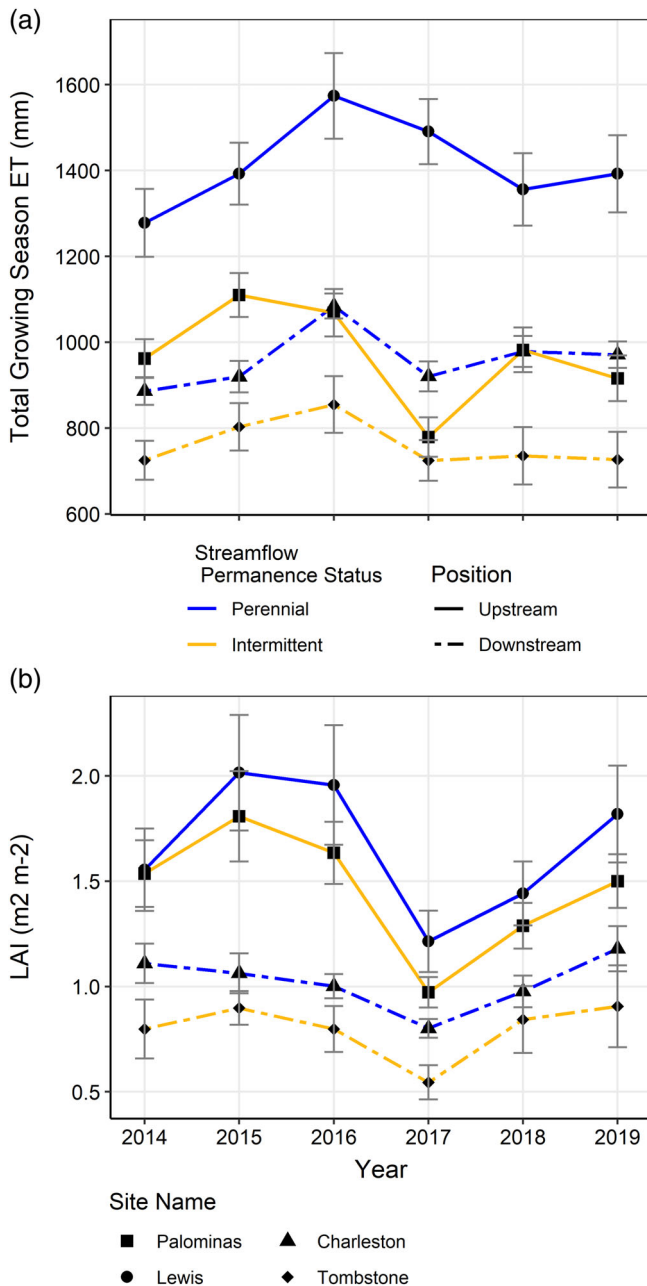


FIGURE 5 Total growing season ET (March 1–Oct 31) and pre-monsoon LAI averaged by stream-sites along the San Pedro River for hydrologic years 2014–2019. Error bars indicate ± 1 SE across 10 sampling polygons per date

climate at landscape scales (Camporeale et al., 2013) and (2) relationships between ecological function and vegetation structure remain constant at landscape scales (Nagler et al., 2009). Across riparian gallery woodland sites in the upper San Pedro River corridor, we found significant differences in the sensitivity of ET to climate variables corresponding with site streamflow permanence (Figure 5, Tables 5 and 6), and the relationships between ET and LAI modelled from remotely sensed data.

Use of independent remote sensing datasets for ET (EEFlux ET_a) and LAI (Landsat 8 NDVI scaled to Landsat 7 NDVI values with field

data-based calibrations) enabled this work to characterize riparian woodland structure–function relationships at riparian corridor scales (10^1 – 10^2 km) over multiple years and a wide range of woodland stand conditions across stream sites. Growing season daily ET rates of 3.0 – 10 mm day⁻¹ for perennial streamflow sites and 2.0 – 6.0 mm day⁻¹ for intermittent-streamflow sites in EEFlux ET_a data overlapped with ranges of previous daily ET rates for cottonwood and willow stands measured by sapflow methods at the Lewis Springs site on the San Pedro River (8 – 12 mm day⁻¹) (Goodrich et al., 2000). Mean growing season total ET ranges calculated for cottonwood-willow riparian woodlands, from 761 (± 184 SE) mm at the intermittent-downstream site (Tombstone) to $1,414$ (± 27 SE) mm at the perennial-flow upstream site (Lewis Springs), were higher than sapflow-based total ET fluxes reported in the past for sites on the San Pedro River (966 mm for perennial-flow Lewis Springs; 484 mm for an intermittent-flow site, Boquillas, closer to Tombstone) (Gazal et al., 2006). Other previously reported total ET ranges for cottonwood-willow included flux tower measurements from the Middle Rio Grande River in New Mexico (850 – $1,150$ mm) (Cleverly et al., 2015), the Cosumnes River “Accidental Forest” in California ($1,095 \pm 30$ mm) (Kochendorfer et al., 2011), and VI-based remote sensing estimates of $1,100$ – $1,300$ mm for cottonwood-willow across the Rio Grande, San Pedro and Lower Colorado rivers (Nagler, Scott, et al., 2005). Given the large range and heterogeneity of riparian woodland stand conditions our sampling polygons covered—including less accessible dense woodland stands—it is reasonable for our methods to result in wider ranges and potentially higher ET values than field studies have been able to quantify.

However, a potential for overestimation of ET for riparian gallery woodlands exists using surface energy-balance remote sensing methods. This is due in part to EEFlux METRIC-model calibration challenges related to the uncertainty of the daily maximum air temperature over well-watered multi-story vegetation canopies, and contributions of ET from understory vegetation or evaporation from moist soils (Senay et al., 2013). A comparison of flux tower-based daily ET against EEFlux daily ET rates for a mesquite woodland near the Charleston stream-site provides evidence that the EEFlux ET_a product has a high absolute value bias, but accurately tracks growing-season ET interannual variability (Figure S7). Similar to methods for VI-based ET remote sensing, where indices (NDVI, or Enhanced Vegetation Index, EVI) are scaled to values for bare soil and canopy maxima (Nagler et al., 2009; Nagler, Scott, et al., 2005), future research could consider use of such scaling techniques for surface energy-balance ET methods to quantify overstorey woodland ET against “background” evaporation from soils. These uncertainties in surface energy-balance ET products for studying natural ecosystems will be important to address as the use of such remote sensing products grows, for example, with the debut of Landsat Provisional Evapotranspiration products from NASA and USGS in 2020 and upcoming OpenET platform in 2021 (<https://etdata.org/>).

The mean LAI values we modelled for stream sites were lower, but overlapped with ranges of past field-measured LAI of natural cottonwood-willow stands (LAI 2 – 3 m² m⁻² along primary stream

TABLE 5 Pearson correlations between total growing season evapotranspiration (ET) and hydro-climate variables for perennial-flow and intermittent-flow stream-sites on the San Pedro River, Arizona for hydrological years 2014–2019

Hydroclimate variable	Season	Total growing season evapotranspiration (ET)							
		Perennial-flow upstream (Lewis Springs)		Perennial-flow downstream (Charleston)		Intermittent-flow upstream (Palominas)		Intermittent-flow upstream (Tombstone)	
		<i>r</i>	<i>p</i>	<i>r</i>	<i>p</i>	<i>r</i>	<i>p</i>	<i>r</i>	<i>p</i>
Temperature - Daily Maximum	Winter	-.129	.808	-.084	.875	.094	.859	.007	.989
	Pre-monsoon	.350	.496	.188	.721	-.313	.546	.050	.924
	Monsoon	.914	.011	.723	.105	.089	.866	.656	.157
Temperature - Daily Minimum	Winter	-.563	.245	-.461	.358	.024	.964	-.380	.457
	Pre-monsoon	-.261	.618	-.396	.437	-.531	.279	-.557	.250
	Monsoon	-.210	.689	-.794	.059 [^]	-.405	.425	-.419	.409
Precipitation ^a	Winter	-.351	.495	-.214	.683	.426	.399	.268	.608
		.251	.631	.381	.456	-.201	.702	.017	.974
	Pre-monsoon	.213	.685	.432	.392	.918	.010	.793	.060 [^]
		.384	.452	.620	.189	.950	.004	.880	.021
	Monsoon	-.351	.495	-.170	.747	.129	.808	-.013	.981
		-.749	.087 [^]	-.517	.294	.423	.404	-.221	.674
Discharge	Winter	NA	NA	-.116	.827	.641	.170	.732	.098 [^]
	Pre-monsoon	NA	NA	.390	.444	.547	.262	.703	.119
	Monsoon	NA	NA	-.575	.233	-.145	.784	-.409	.421

Notes: **Bold red text** indicates significant correlations at $p < .05$. Text with [^] indicates significant correlations at $p < .10$.

^aThe second set of italicized numbers for ET-Precipitation quantify Pearson coefficients and *p*-values using USDA-ARS rain gauges for precipitation data that are closer to stream-sites than the Tombstone-NOAA-COOP climate station. Lewis Springs and Charleston use USDA-ARS gauge 417. Palominas uses gauge 418. Tombstone uses ARS gauge 405. See Figure 1 for geographic locations of rainfall data. ARS rainfall gauge data are available at: <https://www.tucson.ars.ag.gov/dap/digital/aggregate.asp>.

TABLE 6 Pearson correlations between pre-monsoon leaf-area index (LAI) and hydro-climate variables for perennial-flow and intermittent-flow stream-sites on the San Pedro River, Arizona for hydrological years 2014–2019

Hydroclimate variable	Season	Pre-monsoon leaf-area index (LAI)							
		Perennial-flow upstream (Lewis Springs)		Perennial-flow downstream (Charleston)		Intermittent-flow upstream (Palominas)		Intermittent-flow upstream (Tombstone)	
		<i>r</i>	<i>p</i>	<i>r</i>	<i>p</i>	<i>r</i>	<i>p</i>	<i>r</i>	<i>p</i>
Temperature - Daily Maximum	Winter	-.463	.355	-.556	.252	-.281	.589	-.289	.578
	Pre-monsoon	-.626	.184	-.797	.058 [^]	-.597	.211	-.739	.093 [^]
Temperature - Daily Minimum	Winter	-.463	.355	-.265	.612	-.241	.645	-.007	.989
	Pre-monsoon	-.910	.012	-.667	.148	-.765	.076 [^]	-.607	.201
Precipitation ^a	Winter	.538	.271	.181	.731	.481	.334	.386	.450
		.278	.594	.182	.730	-.265	.612	.373	.467
	Pre-monsoon	.919	.010	.418	.409	.859	.028	.707	.116
Discharge	Winter	.695	.125	.083	.876	.834	.039	.476	.340
		NA	NA	.053	.921	.627	.183	.247	.637
	Pre-monsoon	NA	NA	.521	.289	.719	.107	.491	.322

Notes: **Bold red text** indicates significant correlations at $p < .05$. Text with [^] indicates significant correlations at $p < .10$.

^aThe second set of italicized numbers for LAI-Precipitation quantify Pearson coefficients and *p*-values using USDA-ARS rain gauges for precipitation data that are closer to stream-sites than the Tombstone-NOAA-COOP climate station. Lewis Springs and Charleston use USDA-ARS gauge 417. Palominas uses gauge 418. Tombstone uses ARS gauge 405. These rainfall gauge records are available at <https://www.tucson.ars.ag.gov/dap/digital/aggregate.asp>.

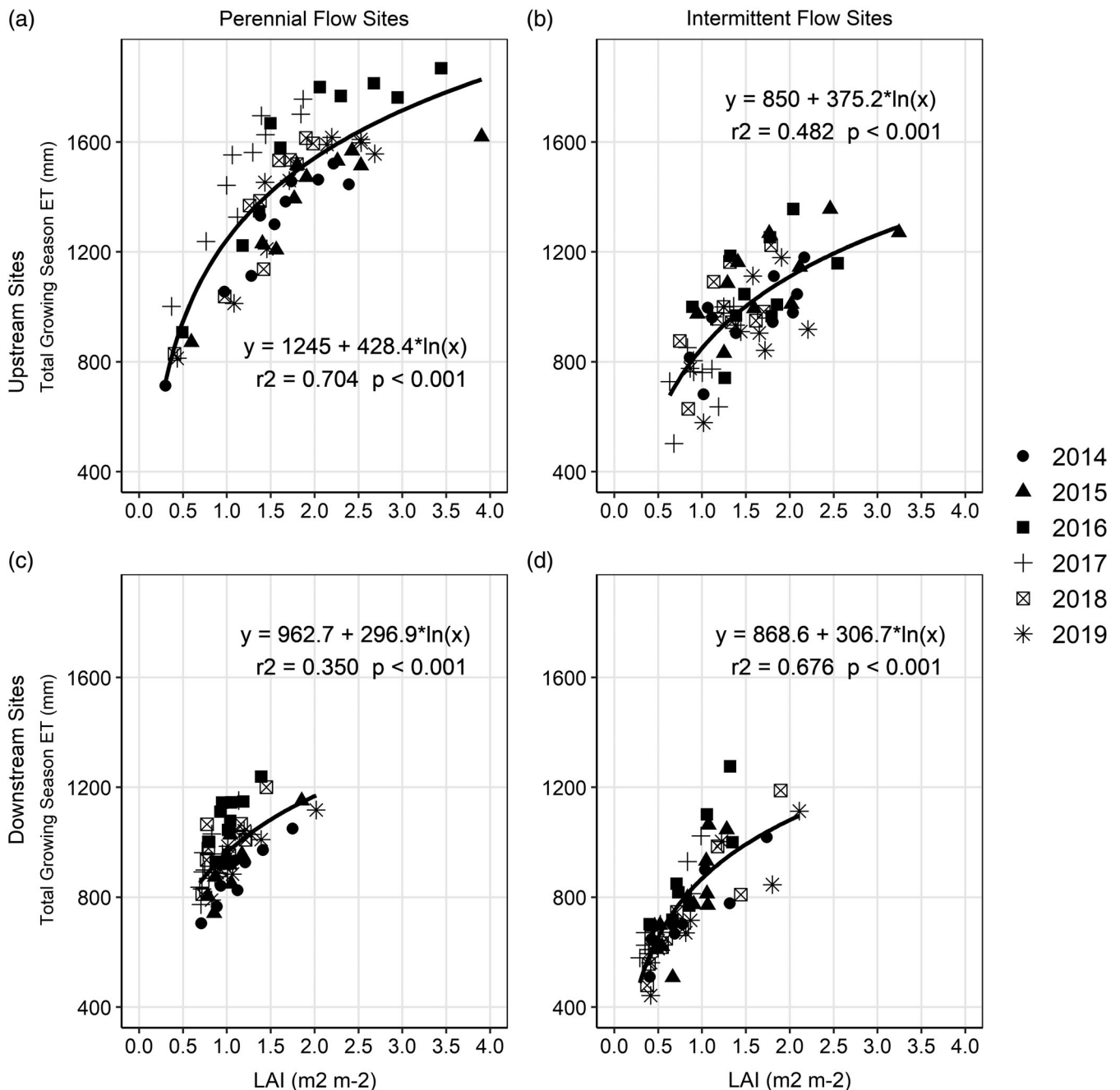


FIGURE 6 Relationships of total growing season ET to LAI for stream sites along the San Pedro River. Panels are organized by streamflow permanence status (columns) and upstream vs. downstream positions (rows). Stream-site names are Lewis Springs (a), Palominas (b), Charleston (c) and Tombstone (d)

channels and $1.5\text{--}2\text{ m}^2\text{ m}^{-2}$ along secondary channels at Lewis Springs during the year 2000 (Farid, Goodrich, Bryant, & Sorooshian, 2008; Schaeffer et al., 2000); LAI of 2.6 at the Cosumnes River (Kochendorfer et al., 2011); LAI of 2–6 on the lower Colorado River (Nagler et al., 2004). Differences in inter-annual LAI trends between upstream and downstream sites are likely due to heterogeneity in vegetation community composition and structure in the polygons we sampled across sites, as well as responses of phenology (leaf-out) to local microclimate conditions. Improved estimation of LAI

from remotely sensed data is an important topic for future research. For example, recent common garden experiments have shown significant differences in canopy architecture for *P. fremontii* from provenance regions with 3–5°C differences in mean annual maximum temperature (Mahoney, Mike, Parker, Lassiter, & Whitham, 2019). Transposing use of LAI-NDVI calibration relationships from the Lower Colorado (with MAMT closer to 30°C) to the cooler San Pedro region (MAMT about 25°C) was necessary for this study because the Lower Colorado relationships were the closest available for this vegetation

type, and measuring LAI in situ was infeasible for this study. Yet this transposition did not account for potential inter-regional differences in canopy structure (e.g., leaf area:stem area ratios) that may affect LAI-NDVI relationships. Thus in future research, there is a need to quantify relationships between light extinction (k) and canopy architectures for riparian vegetation stands across wider sets of geographic and climate regions, in the same way as has been done in the Lower Colorado (Nagler et al., 2004).

Our results corroborated hypothesis 1 of positive correlations between gallery woodland ET and LAI, but they also highlighted significant variations amongst ET-LAI relationships by site. Across the riparian gallery woodlands that we studied spanning perennial and intermittent-flow sites, the spatial variability of ET and LAI exceeded that of inter-annual variability for any particular site. Averaged across all riparian gallery woodland sites (Table 4) the mean spatial CV of ET

was 0.18, nearly twice that of the temporal (inter-annual) CV (0.10). For LAI the comparison was similar, with mean spatial CV of 0.36 versus temporal CV of 0.20.

Different ET-LAI relationships (Figure 6) and ET/LAI ratios by site (Figure 7) suggest there is independent plasticity in vegetation structure and functional traits at stand scales in response to environmental conditions (Eamus et al., 2015; Watson et al., 1999). For example, at Lewis Springs, LAI (canopy structural trait) was positively correlated with pre-monsoon rainfall, but ET (functional trait) was not. Inter-annual ET trends across sites showed more heterogeneity than those of LAI, where all sites showed minimum LAI in the year 2017 with the lowest pre-monsoon rainfall totals (Figure 5). Whilst it was beyond the scope of this study to investigate which specific ecological and plant ecophysiological factors drove the variability in ET-LAI relationships at scales of sampling polygons and stream sites, we posit that differences in species composition, demography, and functional and structural traits at the species level all may contribute to modulate stand-scale ET dynamics. Within the spatial scale of 1–2 stand polygons (100 s m²) we sampled at the Lewis Springs site, significantly higher daily ET rates have been documented for younger successional cottonwood-willow patches on primary stream channels compared to older-successional patches on secondary channels (Schaeffer et al., 2000). As investigated in other global woodlands, trait-based research approaches at the tree species-level are needed to identify what adaptations may be most important for determining stand-level ET-LAI relationships across stream sites with differing water availability (Eamus et al., 2015; Zolfaghar et al., 2014). These findings indicate the importance of accounting for heterogeneity in vegetation structure, function and structure–function relationships at site scales within regional riparian corridors for (1) developing more accurate riparian water budgets and understanding of hydrological processes for local stream reaches across basins, and (2) defining riparian conservation and restoration targets across basins.

To model the implications of variability in vegetation structure (LAI)–function (ET) relationships for estimating riparian water use at riparian corridor scales (10s–100s km), we compared results of using stream site-specific models and a general (all-site) model for estimating ET based on LAI (Table 7). Use of the general model to calculate basin-scale riparian water-requirements would underestimate ET for

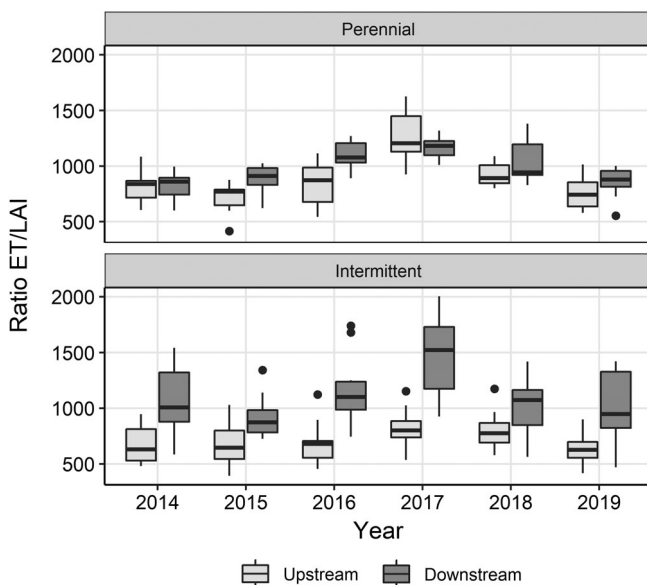


FIGURE 7 Box-plots of ET/LAI ratios for all sampling polygons at perennial and intermittent flow stream-sites along the San Pedro River, 2014–2019. Perennial sites are Lewis Springs (upstream) and Charleston (downstream). Intermittent-flow sites are Palominas (upstream) and Tombstone (downstream)

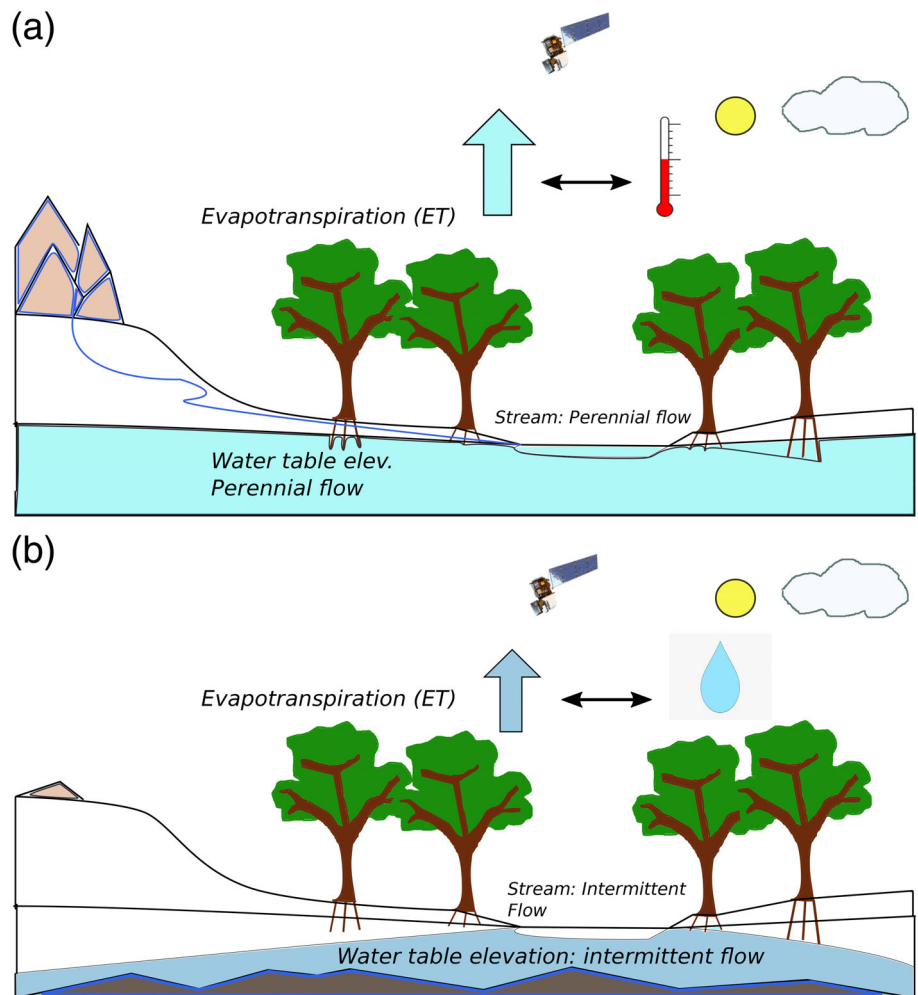
TABLE 7 Total growing season evapotranspiration (ET, in mm) estimated for a canopy LAI range of 1.25–3 at perennial-flow and intermittent-flow stream-sites across the San Pedro River, Arizona

LAI (m ² m ⁻²)	Perennial flow upstream ET (Lewis Springs)	Perennial flow downstream ET (Charleston)	Intermittent-flow upstream ET (Palominas)	Intermittent-flow downstream ET (Tombstone)	All sites pooled
1.25	1,341	1,029	935	937	1,089
1.5	1,419	1,083	1,003	993	1,173
2	1,542	1,169	1,111	1,081	1,306
3	1,716	1,289	1,263	1,206	1,494

Note: All ET values are in mm.

Note: ET estimates listed were calculated for specific stream-sites with site-specific data and logarithmic models shown in Figure 7, and data from all sites pooled using the logarithmic model in Section 3.5.

FIGURE 8 Conceptual diagram summarizing how correlations between cottonwood-willow riparian woodland ET and climate variables relate to streamflow permanence status. (a) At perennial-flow stream-sites, total growing season ET correlated positively with monsoon-season temperature variables. (b) At intermittent-flow stream sites, total growing season ET correlated positively with pre-monsoon rainfall and stream discharge. Provided riparian woodland species composition and structure are comparable, these climate-ET correlations show promise as remote indicators of subsurface water availability relative to overstorey woodland demand



dense riparian stands such as those at Lewis Springs by 15–20% per year, compared to the site-specific model. This could potentially lead to insufficient water allocations in the future in sub-basin scale permitting of ground water extraction. It is likely that riparian vegetation water-use requirements will increase with temperature in the future (Serrat-Capdevila et al., 2011). Such heterogeneity in water requirements at reach scale must be accounted for in conservation planning and water management, especially given the outsized role of large-stature gallery woodlands for biodiversity and ecosystem services.

For the second hypothesis, we found evidence that the sensitivity of overstorey woodland ET to hydroclimate variables differed across sites according to streamflow permanence status. Gallery woodland ET at perennial-flow sites Lewis Springs and Charleston correlated with daily maximum and minimum temperature-related variables. In contrast, precipitation and streamflow-related variables had the strongest correlations with ET at intermittent-flow sites. It was notable that patterns in ET sensitivity to climate showed alignment with stream site flow permanence status, and not vegetation structure (LAI); Lewis Springs, Palominas and Charleston did not differ significantly in terms of their LAI. Yet with similar inter-annual variability in LAI between Lewis Springs and Palominas, Lewis Springs had much higher rates of ET.

Together these findings suggest the possibility of using the sensitivity of gallery woodland ET to climate variables as a remotely sensed indicator of shallow subsurface water availability at reach scales across semi-arid riparian basins (Figure 8). Hydrologic coupling between streamflow and subsurface water resources was strong across all stream sites, especially for winter and dry pre-monsoon seasons (Figure S2), supporting use of streamflow as a proxy for subsurface water availability to overstorey trees. At stream sites with perennial streamflow a combination of variables and hydrologic processes lead to locally positive water balance. These variables and processes include upslope geologic structure, density of surface flow inputs, mountain-block groundwater recharge, floodplain aquifer composition and thickness, and floodplain soil moisture capacity (MacNish et al., 2009). Given isohydric functional tendencies of *Populus* spp., *Salix* spp., other obligate and semi-obligate phreatophytes (Hultine et al., 2020), correlations of gallery woodland ET to maximum daily temperatures in the monsoon season at perennial-flow sites suggest that sufficient subsurface water must be available for woodland trees to keep stomata open for CO₂ assimilation, despite increasing evaporative demand accompanying higher daily temperatures (Figure 8a). In contrast, at sites with intermittent streamflow, where geologic, geomorphologic, or in recent decades potential human influences result in

negative water balance, positive correlations of woodland ET to pre-monsoon rainfall could suggest that subsurface water in the root zone during this less rainy period is limited relative to plant demand (Figure 8b), especially considering lower water table support for such reaches. An important caveat of these interpretations is that up-to-date and accurate information would be necessary to confirm equivalence in vegetation functional traits across sites—to ensure that differences in climate response are not due to differences in species types or disturbance not resolvable at scales of medium-resolution remote sensing. Provided similarity in vegetation types across sites can be confirmed, these differences in climate sensitivity to ET could be mapped at the scale of entire riparian corridors as indicators of reach-scale water availability to overstory woodlands. A change in response to climate variables at one place could be a sign of changing subsurface water-availability conditions, again provided it could be confirmed that the vegetation community itself had not changed in terms of functional traits (e.g., invasive species or exposure of grass after tree-fall, or fire, for example). Updated, accurate information on vegetation species composition and structure from field and remotely sensed data at satellite or near-surface scales (i.e., drone, unmanned aerial system [UAS] imagery) would be valuable to constrain uncertainties in vegetation community composition and structure alongside using vegetation functional response to climate as a subsurface hydrologic indicator.

5 | CONCLUSIONS

In this study, we conducted one of the first riparian corridor-scale assessments of the spatial variability of vegetation structure (LAI)–hydrologic function (ET) relationships in semi-arid riparian gallery woodlands. We found that whilst positive relationships between LAI and ET exist across gallery woodlands at stream sites, there was significant variability in the nature of ET–LAI relationships across sites corresponding with perennial and intermittent flow status. Furthermore, the climate sensitivity of gallery woodland ET differed by stream site water availability—with perennial-flow site ET exhibiting sensitivity to temperature, and intermittent-flow site ET showing sensitivity to pre-monsoon rainfall and stream discharge. These findings indicate the importance of accounting for heterogeneity in vegetation structure, function and structure–function relationships at the reach-scale for (1) developing more precise vegetation demand terms in riparian water budgets for understanding hydrological processes and water balance for local stream reaches across basins, and (2) defining riparian conservation and restoration targets across basins. Additionally, our findings suggest the possibility of using the sensitivity of gallery woodland ET to climate variables as a remote indicator of shallow subsurface water availability at reach scales across semi-arid riparian basins. Future work to address uncertainties in surface energy-balance based remote sensing products, remote estimation of LAI, vegetation species composition and structure, and continued need to collect data on vegetation species, demography and stand structure at

landscape scales are all important to relate our findings to trait-based understandings of riparian vegetation responses to global change.

ACKNOWLEDGEMENTS

This work was funded by the Strategic Environmental Research and Development Program (SERDP) Award RC18-1006, Title “Understanding and Assessing Riparian Habitat Vulnerability to Drought-Prone Climate Regimes on Department of Defence Bases in the Southwestern USA,” P.I. Dr. Michael Singer. We also acknowledge support from The National Science Foundation (BCS-1660490, EAR-1700517 and EAR-1700555). We are honoured to submit this work to Hydrological Processes in the spirit of ecohydrological research motivated by public service that Dr. Edward P. Glenn pioneered throughout his career. We wish we could have collaborated on this paper with him. Dr. Glenn spent several decades of his diverse research career focused on riparian ecosystems of the southwestern U.S. Google Scholar reports over 15,000 citations and 11,200 results for his riparian ecosystem research papers. Just 2 days before his passing in 2017, he was working on a manuscript draft to evaluate changes via satellite observations to the riparian corridor of the San Pedro Riparian National Conservation Area (SPRNCA), the only such national conservation area in the U.S., which was created in 1988 to protect one of the last undammed rivers in this dryland region. Ed would have been proud that this work extended his interests in the region and contributed new methods, findings and discussion about the state of this river in this special issue dedicated to him. Any use of trade, firm, or product names is for descriptive purposes only and does not imply endorsement by the U.S. Government.

DATA AVAILABILITY STATEMENT

Data sources for this study are publicly available and data used for analyses are available from the authors upon request.

ORCID

Marc Mayes  <https://orcid.org/0000-0003-0369-774X>

Michael Bliss Singer  <https://orcid.org/0000-0002-6899-2224>

John C. Stella  <https://orcid.org/0000-0001-6095-7726>

Pamela Nagler  <https://orcid.org/0000-0003-0674-103X>

REFERENCES

- Albright, T. P., Mutiibwa, D., Gerson, A. R., Smith, E. K., Talbot, W. A., O'Neill, J. J., ... Wolf, B. O. (2017). Mapping evaporative water loss in desert passerines reveals an expanding threat of lethal dehydration. *Proceedings of the National Academy of Sciences of the United States of America*, 114(9), 2283–2288. <https://doi.org/10.1073/pnas.1613625114>
- Allen, R., Morton, C., Kamble, B., Kilic, A., Huntington, J., Thau, D., ... Robison, C. (2015). EEFlux: A landsat-based evapotranspiration mapping tool on the Google Earth Engine. Paper presented at the *Joint ASABE/IA Irrigation Symposium 2015: Emerging Technologies for Sustainable Irrigation*, 7004(November), 424–433. Retrieved from <https://doi.org/10.13031/irrig.20152143511>.
- Allen, R. G., Tasumi, M., & Trezza, R. (2007). Satellite-based energy balance for mapping evapotranspiration with internalized calibration

- (METRIC)—model. *Journal of Irrigation and Drainage Engineering*, 133(4), 380–394. [https://doi.org/10.1061/\(ASCE\)0733-9437](https://doi.org/10.1061/(ASCE)0733-9437)
- Anderson, M. C., Hain, C., Wardlow, B., Pimstein, A., Mecikalski, J. R., Kustas, W. P., ... Kustas, W. P. (2011). Evaluation of drought indices based on thermal remote sensing of evapotranspiration over the continental United States. *Journal of Climate*, 24(8), 2025–2044. <https://doi.org/10.1175/2010JCLI3812.1>
- Baldocchi, D., Falge, E., Gu, L., Olson, R., Hollinger, D., Running, S., ... Wofsy, S. (2001). FLUXNET: A new tool to study the temporal and spatial variability of ecosystem-scale carbon dioxide. *Water Vapor, and Energy Flux Densities*, 82, 2415–2434. [https://doi.org/10.1175/1520-0477\(2001\)082<2415:FANTTS>2.3.CO;2](https://doi.org/10.1175/1520-0477(2001)082<2415:FANTTS>2.3.CO;2)
- Bastiaanssen, W. G. M., Noordman, E. J. M., Pelgrum, H., Davids, G., Thoreson, B. P., & Allen, R. G. (2005). SEBAL model with remotely sensed data to improve water-resources management under actual field conditions. *Journal of Irrigation and Drainage Engineering*, 131(1), 85–93. [https://doi.org/10.1061/\(ASCE\)0733-9437](https://doi.org/10.1061/(ASCE)0733-9437)
- Camporeale, C., Perucca, E., Ridolfi, L., & Gurnell, A. M. (2013). Modeling the interactions between river morphodynamics and riparian vegetation. *Reviews of Geophysics*, 51(3), 379–414. <https://doi.org/10.1002/rog.20014>
- Cayan, D. R., Das, T., Pierce, D. W., Barnett, T. P., Tyree, M., & Gershunova, A. (2010). Future dryness in the southwest US and the hydrology of the early 21st century drought. *Proceedings of the National Academy of Sciences of the United States of America*, 107(50), 21271–21276. <https://doi.org/10.1073/pnas.0912391107>
- Cleverly, J., Thibault, J. R., Teet, S. B., Tashjian, P., Hipps, L. E., Dahm, C. N., & Eamus, D. (2015). Flooding regime impacts on radiation, evapotranspiration, and latent energy fluxes over groundwater-dependent riparian cottonwood and saltcedar forests. *Advances in Meteorology*, 2015, 1–14. <https://doi.org/10.1155/2015/935060>
- Dahm, C. N., Cleverly, J. R., Allred Coonrod, J. E., Thibault, J. R., McDonnell, D. E., & Gilroy, D. J. (2002). Evapotranspiration at the land/water interface in a semi-arid drainage basin. *Freshwater Biology*, 47(4), 831–843. <https://doi.org/10.1046/j.1365-2427.2002.00917.x>
- De Cicco, L. A., Hirsch, R. M., Lorenz, D., & Watkins, W. D. (2018). dataRetrieval: R packages for discovering and retrieving water data available from Federal hydrological web services. <https://doi.org/10.5066/P9X4L3GE>
- Diffenbaugh, N. S., Swain, D. L., Touma, D., & Lubchenko, J. (2015). Anthropogenic warming has increased drought risk in California. *Proceedings of the National Academy of Sciences of the United States of America*, 112(13), 3931–3936. <https://doi.org/10.1073/pnas.1422385112>
- Eamus, D., Zolfaghar, S., Villalobos-Vega, R., Cleverly, J., & Huete, A. (2015). Groundwater-dependent ecosystems: Recent insights from satellite and field-based studies. *Hydrology and Earth System*, 19, 4229–4256. <https://doi.org/10.5194/hess-19-4229-2015>
- Ekstrom, C. T. (2019). MESS: Miscellaneous esoteric statistical scripts. Retrieved from <https://cran.r-project.org/package=MESS>.
- Farid, A., Goodrich, D. C., Bryant, R., & Sorooshian, S. (2008, January 1). Using airborne lidar to predict leaf area index in cottonwood trees and refine riparian water-use estimates. *Journal of Arid Environments*, 72(1), 1–15. <https://doi.org/10.1016/j.jaridenv.2007.04.010>
- Gazal, R. M., Scott, R. L., Goodrich, D. C., & Williams, D. G. (2006). Controls on transpiration in a semiarid riparian cottonwood forest. *Agricultural and Forest Meteorology*, 137(1–2), 56–67. <https://doi.org/10.1016/J.AGRFORMET.2006.03.002>
- Glenn, E. P., Nagler, P. L., & Huete, A. R. (2010). Vegetation index methods for estimating evapotranspiration by remote sensing. *Surveys in Geophysics*, 31(6), 531–555. <https://doi.org/10.1007/s10712-010-9102-2>
- Goodrich, D. C., Scott, R., Qi, J., Goff, B., Unkrich, C. L., Moran, M. S., Ni, W., & (2000). Seasonal estimates of riparian evapotranspiration using remote and in situ measurements. In *Agricultural and Forest Meteorology*, 105, 281–309. [https://doi.org/10.1016/S0168-1923\(00\)00197-0](https://doi.org/10.1016/S0168-1923(00)00197-0)
- Goodrich, D. C., Unkrich, C. L., Keefer, T. O., Nichols, M. H., Stone, J. J., Levick, L. R., & Scott, R. L. (2008). Event to multidecadal persistence in rainfall and runoff in Southeast Arizona. *Water Resources Research*, 44(5), 1–17. <https://doi.org/10.1029/2007WR006222>
- Grime, J. P. (1977). Evidence for the existence of three primary strategies in plants and its relevance to ecological and evolutionary theory. *The American Naturalist*, 111(982), 1169–1194. <https://doi.org/10.1086/283244>
- Gungle, B., Callegary, J. B., Paretti, N. V., Kennedy, J. R., Eastoe, C. J., Turner, D. S., ... Sugg, Z. P. (2019). Hydrological conditions and evaluation of sustainable groundwater use in the Sierra Vista subwatershed, upper San Pedro Basin, Southeastern Arizona. USGS Scientific Investigations Report 2016-5114. Reston, VA. Retrieved from <https://doi.org/10.3133/sir20165114>.
- Hultine, K. R., Bush, S. E., & Ehleringer, J. R. (2010). Ecophysiology of riparian cottonwood and willow before, during, and after two years of soil water removal. *Ecological Applications*, 20. Retrieved from, 347–361. <https://esajournals.onlinelibrary.wiley.com/doi/pdf/10.1890/09-0492.1>
- Hultine, K. R., Froend, R., Blasini, D., Bush, S. E., Karlinski, M., & Koepke, D. F. (2020). Hydraulic traits that buffer deep-rooted plants from changes in hydrology and climate. *Hydrological Processes*, 34(2), 209–222. <https://doi.org/10.1002/hyp.13587>
- Irmak, S., Kabenge, I., Rudnick, D., Knezevic, S., Woodward, D., & Moravek, M. (2013). Evapotranspiration crop coefficients for mixed riparian plant community and transpiration crop coefficients for common reed, cottonwood and peach-leaf willow in the Platte River basin, Nebraska-USA. *Journal of Hydrology*, 481, 177–190. <https://doi.org/10.1016/j.jhydrol.2012.12.032>
- Jones, K. B., Slonecker, E. T., Nash, M. S., Neale, A. C., Wade, T. G., & Hamann, S. (2010). Riparian habitat changes across the continental United States (1972–2003) and potential implications for sustaining ecosystem services. *Landscape Ecology*, 25(8), 1261–1275. <https://doi.org/10.1007/s10980-010-9510-1>
- Kabenge, I., & Irmak, S. (2012). Evaporative losses from a common reed-dominated peachleaf willow and cottonwood riparian plant community. *Water Resources Research*, 48(9), 1–17. <https://doi.org/10.1029/2012WR011902>
- Kochendorfer, J., Castillo, E. G., Haas, E., Oechel, W. C., Paw, U., & T, K. (2011). Net ecosystem exchange, evapotranspiration and canopy conductance in a riparian forest. *Agricultural and Forest Meteorology*, 151, 544–553. <https://doi.org/10.1016/j.agrformet.2010.12.012>
- Krueper, D., Bart, J., & Rich, T. D. (2003). Response of vegetation and breeding birds to the removal of cattle on the San Pedro River, Arizona (U.S.A.). *Conservation Biology*, 17(2), 607–615. <https://doi.org/10.1046/j.1523-1739.2003.01546.x>
- Leenhouts, J., Stromberg, J. C., & Scott, R. L. (2006). *Hydrologic requirements of and consumptive ground-water use by riparian vegetation along the San Pedro River, Arizona*. USGS-Scientific Investigations Report (Vol. 2005-5163). Reston, VA: United States Department of the Interior, US Geological Survey.
- Leenhouts, J. M. (2006). Hydrology of the San Pedro riparian National Conservation Area, Arizona. In J. Leenhouts, J. C. Stromberg, & R. L. Scott (Eds.), *Hydrologic requirements of and consumptive ground-water use by riparian vegetation along the San Pedro River, Arizona* (pp. 23–75). Reston, VA: U.S. Geological Survey.
- MacNish, R., Baird, K. J., & Maddock, T., III (2009). Groundwater hydrology of the San Pedro River basin. In J. C. Stromberg & B. Tellman (Eds.), *Ecology and conservation of the San Pedro River* (pp. 285–299). Tucson, AZ: The University of Arizona Press.
- Mahoney, S. M., Mike, J. B., Parker, J. M., Lassiter, L. S., & Whitham, T. G. (2019). Selection for genetics-based architecture traits in a native

- cottonwood negatively affects invasive tamarisk in a restoration field trial. *Restoration Ecology*, 27(1), 15–22. <https://doi.org/10.1111/rec.12840>
- Makings, E. (2005). Flora of the San Pedro riparian National Conservation Area, Cochise County, Arizona. *USDA Forest Service Proceedings*, 36, 92–99.
- Mangiafico, S. (2020). Functions to support extension education program evaluation. Retrieved from <https://rcompanion.org/handbook/>.
- McDowell, N., Pockman, W. T., Allen, C. D., Breshears, D. D., Cobb, N., Kolb, T., ... Yezpe, E. A. (2008). Mechanisms of plant survival and mortality during drought: Why do some plants survive while others succumb to drought? *New Phytologist*, 178(4), 719–739. <https://doi.org/10.1111/j.1469-8137.2008.02436.x>
- McLaughlin, B. C., Ackerly, D. D., Klos, P. Z., Natali, J., Dawson, T. E., & Thompson, S. E. (2017). Hydrologic refugia, plants, and climate change. *Global Change Biology*, 23(8), 2941–2961. <https://doi.org/10.1111/gcb.13629>
- Nagler, P. L., Cleverly, J., Glenn, E., Lampkin, D., Huete, A., & Wan, Z. (2005). Predicting riparian evapotranspiration from MODIS vegetation indices and meteorological data. *Remote Sensing of Environment*, 94, 17–30. <https://doi.org/10.1016/j.rse.2004.08.009>
- Nagler, P. L., Glenn, E. P., Lewis Thompson, T., & Huete, A. (2004). Leaf area index and normalized difference vegetation index as predictors of canopy characteristics and light interception by riparian species on the lower Colorado River. *Agricultural and Forest Meteorology*, 125, 1–17. <https://doi.org/10.1016/j.agrformet.2004.03.008>
- Nagler, P. L., Morino, K., Murray, R. S., Osterberg, J., & Glenn, E. P. (2009). An empirical algorithm for estimating agricultural and riparian evapotranspiration using MODIS enhanced vegetation index and ground measurements of ET. I. Description of method. *Remote Sensing*, 1(4), 1273–1297. <https://doi.org/10.3390/rs1041273>
- Nagler, P. L., Scott, R. L., Westenburg, C., Cleverly, J. R., Glenn, E. P., & Huete, A. R. (2005). Evapotranspiration on western U.S. rivers estimated using the enhanced vegetation index from MODIS and data from eddy covariance and Bowen ratio flux towers. *Remote Sensing of Environment*, 97, 337–351. <https://doi.org/10.1016/j.rse.2005.05.011>
- Nguyen, U., Glenn, E. P., Nagler, P. L., & Scott, R. L. (2015). Long-term decrease in satellite vegetation indices in response to environmental variables in an iconic desert riparian ecosystem: The upper San Pedro, Arizona, United States. *Ecohydrology*, 8(4), 610–625. <https://doi.org/10.1002/eco.1529>
- Ohmart, R. D., Anderson, B. W., & Hunter, W. C. (1988). *The ecology of the lower Colorado River from Davis dam to the Mexico-United States international boundary: A community profile*. Washington, DC: US Department of the Interior, US Fish and Wildlife Service.
- Perry, L. G., Reynolds, L. V., Beechie, T. J., Collins, M. J., & Shafroth, P. B. (2015). Incorporating climate change projections into riparian restoration planning and design. *Ecohydrology*, 8(5), 863–879. <https://doi.org/10.1002/eco.1645>
- Polade, S. D., Gershunov, A., Cayan, D. R., Dettinger, M. D., & Pierce, D. W. (2017). Precipitation in a warming world: Assessing projected hydro-climate changes in California and other Mediterranean climate regions. *Scientific Reports*, 7(1), 1–10. <https://doi.org/10.1038/s41598-017-11285-y>
- Ramírez-Hernández, J., Rodríguez-Burgueño, J. E., Zamora-Arroyo, F., Carreón-Díazconti, C., & Pérez-González, D. (2015). Mimic pulse-base flows and groundwater in a regulated river in semiarid land: Riparian restoration issues. *Ecological Engineering*, 83, 239–248. <https://doi.org/10.1016/j.ecoleng.2015.06.006>
- Schaeffer, S. M., Williams, D. G., & Goodrich, D. C. (2000). Transpiration of cottonwood/willow forest estimated from sap flux. *Agricultural and Forest Meteorology*, 105, 257–270. [https://doi.org/10.1016/S0168-1923\(00\)00186-6](https://doi.org/10.1016/S0168-1923(00)00186-6)
- Schlatter, K. J., Grabau, M. R., Shafroth, P. B., & Zamora-Arroyo, F. (2017). Integrating active restoration with environmental flows to improve native riparian tree establishment in the Colorado River Delta. *Ecological Engineering*, 106, 661–674. <https://doi.org/10.1016/j.ecoleng.2017.02.015>
- Scott, R. L., Cable, W. L., Huxman, T. E., Nagler, P. L., Hernandez, M., & Goodrich, D. C. (2008). Multiyear riparian evapotranspiration and groundwater use for a semiarid watershed. *Journal of Arid Environments*, 72(7), 1232–1246. <https://doi.org/10.1016/j.jaridenv.2008.01.001>
- Seager, R., Ting, M., Held, I., Kushnir, Y., Lu, J., Vecchi, G., ... Naik, N. (2007). Model projections of an imminent transition to a more arid climate in southwestern North America. *Science*, 316(5828), 1181–1184. <https://doi.org/10.1126/science.1139601>
- Seavy, N. E., Gardali, T., Golet, G. H., Griggs, F. T., Howell, C. A., Kelsey, R., ... Weigand, J. F. (2009). Why climate change makes riparian restoration more important than ever: Recommendations for practice and research. *Ecological Restoration*, 27(3), 330–338. <https://doi.org/10.3368/er.27.3.330>
- Senay, G. B. (2018). Satellite Psychrometric formulation of the operational simplified surface energy balance (SSEBop) model for quantifying and mapping evapotranspiration. *Applied Engineering in Agriculture*, 34(3), 555–566. <https://doi.org/10.13031/aea.12614>
- Senay, G. B., Bohms, S., Singh, R. K., Gowda, P. H., Velpuri, N. M., Alemu, H., & Verdin, J. P. (2013). Operational evapotranspiration mapping using remote sensing and weather datasets: A new parameterization for the SSEB approach. *Journal of the American Water Resources Association*, 49(3), 577–591. <https://doi.org/10.1111/jawr.12057>
- Serrat-Capdevila, A., Scott, R. L., James Shuttleworth, W., & Valdés, J. B. (2011). Estimating evapotranspiration under warmer climates: Insights from a semi-arid riparian system. *Journal of Hydrology*, 399(1–2), 1–11. <https://doi.org/10.1016/j.jhydrol.2010.12.021>
- Shafroth, P. B., Stromberg, J. C., & Patten, D. T. (2002). Woody riparian vegetation response to different alluvial water table regimes. *Western North American Naturalist*, 60(1), 66–76. <https://scholarsarchive.byu.edu/cgi/viewcontent.cgi?article=1094&context=wnan>
- Singer, M. B., & Michaelides, K. (2017). Deciphering the expression of climate change within the lower Colorado River basin by stochastic simulation of convective rainfall. *Environmental Research Letters*, 12(10), 1–10. <https://doi.org/10.1088/1748-9326/aa8e50>
- Singer, M. B., Sargeant, C. I., Piégay, H., Riquier, J., Wilson, R. J. S., & Evans, C. M. (2014). Floodplain ecohydrology: Climatic, anthropogenic, and local physical controls on partitioning of water sources to riparian trees. *Water Resources Research*, 50(5), 4490–4513. <https://doi.org/10.1002/2014WR015581>
- Smith, S. D., Devitt, D. A., Sala, A., Cleverly, J. R., & Busch, D. E. (1998). Water relations of riparian plants from warm desert regions. *Wetlands*, 18(4), 687–696. <https://doi.org/10.1007/BF03161683>
- Stella, J. C., & Bendix, J. (2018). Multiple stressors in riparian ecosystems. In *Multiple stressors in river ecosystems: Status, impacts and prospects for the future* (pp. 81–110). Cambridge, MA: Elsevier. <https://doi.org/10.1016/B978-0-12-811713-2.00005-4>
- Stella, J. C., Riddle, J., Piégay, H., Gagnage, M., & Trémélo, M. L. (2013). Climate and local geomorphic interactions drive patterns of riparian forest decline along a Mediterranean Basin river. *Geomorphology*, 202, 101–114. <https://doi.org/10.1016/j.geomorph.2013.01.013>
- Stella, J. C., Rodríguez-González, P. M., Dufour, S., & Bendix, J. (2013). Riparian vegetation research in Mediterranean-climate regions: Common patterns, ecological processes, and considerations for management. In *Hydrobiologia*. 719(2013), 291–315. <https://doi.org/10.1007/s10750-012-1304-9>
- Stromberg, J. C., Lite, S. J., Dixon, M., Rychener, T., & Makings, E. (2006). Relations between Streamflow regime and riparian vegetation composition, structure, and diversity within the San Pedro riparian National

- Conservation Area, Arizona. In J. M. Leenhouts, J. C. Stromberg, & R. L. Scott (Eds.), *Hydrologic requirements of and consumptive groundwater use by riparian vegetation along the San Pedro River, Arizona* (pp. 77–106). Reston, VA: U.S. Geological Survey.
- Stromberg, J. C., Lite, S. J., Rychener, T. J., Levick, L. R., Dixon, M. D., & Watts, J. M. (2006). Status of the riparian ecosystem in the upper San Pedro River, Arizona: Application of an assessment model. *Environmental Monitoring and Assessment*, 115(1–3), 145–173, 173. <https://doi.org/10.1007/s10661-006-6549-1>
- Stromberg, J. C., Tluczek, M. G. F., Hazelton, A. F., & Ajami, H. (2010). A century of riparian forest expansion following extreme disturbance: Spatio-temporal change in Populus/Salix/Tamarix forests along the upper San Pedro River, Arizona, USA. *Forest Ecology and Management*, 259(6), 1181–1189. <https://doi.org/10.1016/j.foreco.2010.01.005>
- Thomas, B. E., & Pool, D. R. (2006). In *Trends in streamflow of the San Pedro River, southeastern Arizona, and regional trends in precipitation and streamflow in southeastern Arizona and southwestern New Mexico*, Reston, VA: US Department of Interior, US Geological Survey. <https://doi.org/10.3133/pp1712>
- Watson, F. G. R., Vertessy, R. A., & Grayson, R. B. (1999). Large-scale modeling of forest hydrological processes and their long-term effect on water yield. *Hydrological Processes*, 13(5), 689–700. [https://doi.org/10.1002/\(SICI\)1099-1085\(19990415\)13:5<689::AID-HYP773>3.0.CO;2-D](https://doi.org/10.1002/(SICI)1099-1085(19990415)13:5<689::AID-HYP773>3.0.CO;2-D)
- Williams, D., & Scott, R. L. (2009). Vegetation-hydrology interactions: Dynamics of riparian plant water use. Juliet C. Stromberg & Barbara Tellman (Eds.), In *Ecology and conservation of the San Pedro River* (pp. 37–56). Tuscon, AZ: University of Arizona Press.
- Wilson, J. L., & Guan, H. (2004). Mountain-block hydrology and mountain-front recharge. In J. F. Hogan, F. M. Phillips, & B. R. Scanlon (Eds.), *Groundwater recharge in a desert environment: The southwestern United States* (pp. 113–138). Washington, DC: American Geophysical Union.
- Zhang, K., Kimball, J. S., Nemani, R. R., Running, S. W., Hong, Y., Gourley, J. J., & Yu, Z. (2015). Vegetation greening and climate change promote multidecadal rises of global land evapotranspiration. *Scientific Reports*, 5(1), 1–9. <https://doi.org/10.1038/srep15956>
- Zolfaghar, S., Villalobos-Vega, R., Cleverly, J., Zeppel, M., Rumman, R., & Eamus, D. (2014). The influence of depth-to-groundwater on structure and productivity of eucalyptus woodlands. *Australian Journal of Botany*, 62(5), 428. <https://doi.org/10.1071/BT14139>

SUPPORTING INFORMATION

Additional supporting information may be found online in the Supporting Information section at the end of this article.

How to cite this article: Mayes M, Caylor KK, Singer MB, Stella JC, Roberts D, Nagler P. Climate sensitivity of water use by riparian woodlands at landscape scales. *Hydrological Processes*. 2020;34:4884–4903. <https://doi.org/10.1002/hyp.13942>